

AdaTerm: Adaptive T-Distribution Estimated Robust Moments towards Noise-Robust Stochastic Gradient Optimizer

Wendyam Eric Lionel Ilboudo^{*1} Taisuke Kobayashi^{*1} Kenji Sugimoto¹

Abstract

As the problems to be optimized with deep learning become more practical, their datasets inevitably contain a variety of noise, such as mislabeling and substitution by estimated inputs/outputs, which would have negative impacts on the optimization results. As a safety net, it is a natural idea to improve a stochastic gradient descent (SGD) optimizer, which updates the network parameters as the final process of learning, to be more robust to noise. The related work revealed that the first momentum utilized in the Adam-like SGD optimizers can be modified based on the noise-robust student's t-distribution, resulting in inheriting the robustness to noise. In this paper, we propose AdaTerm, which derives not only the first momentum but also all the involved statistics based on the student's t-distribution. If the computed gradients seem to probably be aberrant, AdaTerm is expected to exclude the computed gradients for updates, and reinforce the robustness for the next updates; otherwise, it updates the network parameters normally, and can relax the robustness for the next updates. With this noise-adaptive behavior, the excellent learning performance of AdaTerm was confirmed via typical optimization problems with several cases where the noise ratio would be different.

technique for a given optimization problem. Therefore, in parallel with the development of various network structures like residual networks (He et al., 2016), various optimizers that can optimize the networks in a more stable and efficient manner have been pursued. The most representative optimizer would be Adam (Kingma & Ba, 2014), and a lot of its variants with respective features have been proposed (see the survey for details (Sun et al., 2019; Schmidt et al., 2021)). Among them, in our knowledge, RAdam (Liu et al., 2020) and AdaBelief (Zhuang et al., 2020) have illustrated the state-of-the-art learning performance.

One of the features of the SGD optimizers is robustness to noise in gradients, which can result for example from the use of noisy datasets with mislabeling (Mirylenka et al., 2017; Suchi et al., 2019) and from optimization problems that require the use of estimated inputs and/or outputs like long-term dynamics learning (Chen et al., 2018; Kishida et al., 2020), reinforcement learning (RL) (Sutton & Barto, 2018), and distillation from the trained teacher(s) (Rusu et al., 2015; Gou et al., 2021). This feature is essential in robot learning problems, where the available dataset is small and the adverse effects of noise are easily apparent. Not only that, but it has been shown empirically in (Simsekli et al., 2019) and (Zhou et al., 2020) that the norm of the gradient noise in both Adam and SGD had heavy tails, even in the absence of label noise. Previous studies have gained the robustness to noise ability in such cases mainly by detecting and excluding the aberrant gradients affected by noise (Gulcehre et al., 2017; Holland & Ikeda, 2019; Prasad et al., 2020; Kim & Choi, 2021), as summarized in (Ilboudo et al., 2020).

In order to make the SGD optimizers robust to such noise, the related work (Ilboudo et al., 2020) has focused on the fact that the first momentum used in the recent Adam-like optimizers is computed with exponential moving average, which can be regarded as the mean of normal distribution that is sensitive to noises. By converting such a noise-sensitive first momentum into the t-momentum — derived from the student's t-distribution — which is robust to noise, most of the Adam-like optimizers can acquire robustness. In addition, the hyper-parameter of the t-momentum (i.e. the degrees of freedom) which determines the level of robust-

1. Introduction

Deep learning (LeCun et al., 2015) is one of the most successful technologies in the last decade. It employs stochastic gradient descent (SGD) optimizer (Robbins & Monro, 1951) to optimize deep neural networks using first-order gradients over network parameters obtained by a back-propagation

^{*}Equal contribution ¹Division of Information Science, Nara Institute of Science and Technology, Nara, Japan. Correspondence to: Wendyam Eric Lionel Ilboudo <ilboudo.wendyam_eric.in1@is.naist.jp>, Taisuke Kobayashi <kobayashi@is.naist.jp>, Kenji Sugimoto <kenji@is.naist.jp>.

ness can, as shown in a recent work (Ilboudo et al., 2021), be tuned automatically by combining it with a heuristic estimation method. As a result, the latest version, At-Adam, has acquired adaptive behaviors to the noise ratio in the problem to be solved while suppressing excessive robustness.

However, the above optimizer modifies only the first momentum, and the second momentum, which is also usually in the Adam-like optimizers, is updated by the basic exponential moving average. Although its smoothness parameter β_2 is large and can reduce the effects of noise as mentioned in the literature (Ilboudo et al., 2020), such design induces a discrepancy in assumptions. Similarly, although the latest optimizer makes the degrees of freedom adjustable, it is unclear whether the heuristic adjustment violates the other assumptions and/or interferes with the other parts of the algorithm. In the end, the lack of a unified derivation of the algorithm as a noise-robust optimizer would allow potential problems to be included.

This paper proposes *Adaptive T-distribution estimated robust moments*, called AdaTerm, with a unified derivation of all the sample statistics based on their gradients for maximum likelihood estimation of the student’s t-distribution. Since the gradient-based update of the statistics may violate their respective domains, AdaTerm surrogates them by their upper bounds if necessary, and introduces adaptive step sizes that make the updates be an interpolation between the past statistics values and the update amounts. Such adaptive step sizes also allow the smoothness parameters β to be common for all the involved statistics. In addition, since the gradient of the degrees of freedom in the multi-dimensional case has been reported to not be consistent with our expectation (briefly it is too small, see details in (Ley & Neven, 2012)), it is appropriately approximated as in the one-dimensional case where our expectation holds. This approximated value can also be used as the upper bound. As expected, AdaTerm can obtain the following qualitative behaviors from the above implementations: if the given gradients are considered aberrant, it reinforces the robustness while excluding the gradients; otherwise, it relaxes the robustness to facilitate updates.

Our contributions in this paper are four folds:

1. Unified derivation of a novel SGD algorithm that is adaptively robust to noise
2. Easing the difficulty of tuning hyper-parameters by using a common smoothness parameter for all the statistics
3. Theoretical proof of the regret bound (see Appendix B)
4. Numerical verification of usefulness in major test functions and typical problems (i.e. classification problems

with mislabeling, long-term prediction problems, reinforcement learning, and policy distillation)

In the last verification, we compared not only AdaBelief and RAdam as the state-of-the-art algorithms but also t-Adam variants developed in the related work.

2. Problem statement

2.1. Optimization problem solved by SGD optimizer

Let us briefly define the optimization (minimization without loss of generality) problem that we will solve using either of the SGD optimizers. Suppose that input data x and output data y are generated according to the problem-specific (stochastic) rule, $p(x, y)$, the problem-specific minimization target, \mathcal{L} , is given as follows:

$$\mathcal{L} = \mathbb{E}_{x, y \sim p(x, y)} [\ell(f(x; \theta), y)] \quad (1)$$

where ℓ denotes the loss function for each data, and $f(x; \theta)$ denotes the mapping function (e.g. from x to y) with the parameter set θ which is optimized through this minimization.

The above expectation operation can be approximated by Monte Carlo method. In other words, a dataset containing N pairs of (x, y) , $\mathcal{D} = \{(x_n, y_n)\}_{n=1}^N$, is constructed according to the problem-specific rule. With \mathcal{D} , the above minimization target is replaced as follows:

$$\mathcal{L}_{\mathcal{D}} = \frac{1}{|\mathcal{D}|} \sum_{x_n, y_n \in \mathcal{D}} \ell(f(x_n; \theta), y_n) \quad (2)$$

where $|\mathcal{D}|$ denotes the size of dataset (N in this case).

We can then compute the gradient w.r.t. θ , $g = \nabla_{\theta} \mathcal{L}_{\mathcal{D}}$, and use gradient descent to obtain the (sub)optimal θ that (locally) minimizes $\mathcal{L}_{\mathcal{D}}$. However, if \mathcal{D} is large, the above gradient computation would be infeasible due to the limitation of computational resources. The SGD optimizer (Robbins & Monro, 1951) therefore extracts a subset (a.k.a. mini batch) at each update step t , $\mathcal{B}_t \subset \mathcal{D}$, and updates θ from θ_{t-1} to θ_t as follows:

$$g_t = \nabla_{\theta_{t-1}} \mathcal{L}_{\mathcal{B}_t} \quad (3)$$

$$\theta_t = \theta_{t-1} - \alpha \eta(g_t) \quad (4)$$

where $\alpha > 0$ denotes the learning rate, and η denotes the function to modify g_t to improve the learning performance. Namely, various SGD optimizers have their own η .

For example, in the case of Adam (Kingma & Ba, 2014), which is the most popular optimizer in recent years, η is given with three hyper-parameters, $\beta_1 \in (0, 1)$, $\beta_2 \in (0, 1)$, and $\epsilon \ll 1$.

$$\eta^{\text{Adam}}(g_t) = \frac{m_t(1 - \beta_1^t)^{-1}}{\sqrt{v_t(1 - \beta_2^t)^{-1} + \epsilon}} \quad (5)$$

where

$$m_t = \beta_1 m_{t-1} + (1 - \beta_1) g_t \quad (6)$$

$$v_t = \beta_2 v_{t-1} + (1 - \beta_2) g_t^2 \quad (7)$$

Adam can be simply interpreted that, since g_t fluctuates depending on how \mathcal{B}_t is sampled, the first momentum m_t smoothes g_t with the past gradients to stabilize the update, and the second momentum v_t scales g_t , which is different depending on the problem, to increase the generality.

2.2. Inaccurate datasets in practical cases

If the above problem setting is satisfied, we can stably acquire one of the local solutions through one of the SGD optimizers, although their regret bounds may be different (Reddi et al., 2018; Alacaoglu et al., 2020). However, in real problems, it is difficult to make datasets that follow the problem-specific rules exactly.

For example, in RL (Sutton & Barto, 2018), the optimal actions for tasks cannot be explicitly defined, so an agent learns the policy (i.e. mapping from state inputs to action outputs) by estimating the optimal actions based on reward values given from the tasks. When distilling knowledge and skills from trained large-scale models to a smaller one (Gou et al., 2021), biases resulting in training will prevent the generation of accurate supervised signals. In the problem of learning dynamics from time-series data, the long-term prediction accuracy may be involved in the loss function with predicted values as inputs (Chen et al., 2018). Even in classification problems, it is not realistic to expect all the data to be correctly labelled, especially when employing (semi-)automatic annotation techniques (Suchi et al., 2019).

All of the above examples can be interpreted as the problem of learning with an inaccurate dataset $\tilde{\mathcal{D}} = \mathcal{D} \cup \mathcal{E}$ with a noisy dataset, $\mathcal{E} \not\subseteq \mathcal{D}$, caused by the estimated values, mislabeling, and so on. Please note that the optimization for \mathcal{D} would be impossible if $|\mathcal{D}| < |\mathcal{E}|$ since the majority is switched; hence, we assume $|\mathcal{D}| > |\mathcal{E}|$.

3. Derivation of AdaTerm

3.1. Overview

Since the gradient for \mathcal{E} is disturbed, this paper develops a noise-robust optimizer to achieve learning along \mathcal{D} while properly detecting and excluding such disturbed gradient as noise. Although it is possible to make the loss function ℓ noise-robust, e.g. (Ma et al., 2020), the noise-robust optimizer proposed in this paper is highly useful in that it can be employed very widely as a safety net.

In order to exclude the above disturbed gradients, we assume that the gradients g can be modeled by the student's t-distribution, which has a heavy tail and is robust to out-

liers, referring to the related work (Ilboudo et al., 2020). Note that this assumption is acceptable because it has been empirically shown that the norm of the noise has heavy tails (Simsekli et al., 2019) and (Zhou et al., 2020). Specifically, g is assumed to be generated from the d -dimensional diagonal student's t-distribution with three kinds of sample statistics: a location parameter $m \in \mathbb{R}^d$; a scale parameter $v \in \mathbb{R}_{>0}^d$; and degrees of freedom $\nu \in \mathbb{R}_{>0}$.

$$g \sim \frac{\Gamma(\frac{\nu+d}{2})}{\Gamma(\frac{\nu}{2})(\nu\pi)^{\frac{d}{2}} \prod_d \sqrt{v_d}} \left(1 + \frac{1}{\nu} \sum_d (g_d - m_d)^2 v_d^{-1} \right)^{-\frac{\nu+d}{2}} \\ =: \mathcal{T}(g \mid m, v, \nu) \quad (8)$$

where Γ denotes the gamma function. d corresponds to the dimension size of each subset of parameters: that means, following the related work (Ilboudo et al., 2020) and PyTorch implementation (Paszke et al., 2017), AdaTerm is applied to a weight matrix and a bias in each layer separately.

In the paper (Ilboudo et al., 2020), only m has been estimated based on its maximum likelihood solution, and in a later paper (Ilboudo et al., 2021), ν has been adjusted by a heuristic approximation of the maximum likelihood (Aeschliman et al., 2010). This paper simultaneously estimates m , v , and ν based on their surrogated gradients to maximize the log-likelihood. The unified derivation yields a more adaptive ν (see 4), with the same computational complexity (i.e. $\mathcal{O}(d)$) as the other major optimizers. The detailed derivation is described below, and the pseudocode of AdaTerm is summarized as Alg. 1 in Appendix A. The regret bound is also analyzed in Appendix B.

3.2. Gradients for maximum log-likelihood

To derive AdaTerm, let us consider the problem of maximizing the log-likelihood, $\ln \mathcal{T}(g \mid m, v, \nu)$, in order to estimate m , v , and ν that can adequately model the recent g . Since this model is expected to be time-varying, we simply employ a gradient ascent at each step instead of optimization by EM algorithm (Lange et al., 1989; Doğru et al., 2018), which comes with high computational cost. In addition, as will be explained later, the pure gradients of v and ν does not provide the expected behavior, hence their surrogated versions are introduced.

Nevertheless, we first show the pure gradient for each statistic. To simplify the notation, the following variables are defined.

$$s = (g - m)^2, \quad D = \frac{1}{d} s^\top v^{-1}, \quad \tilde{\nu} = \nu d^{-1}, \quad w_{mv} = \frac{\tilde{\nu} + 1}{\tilde{\nu} + D}$$

When ν is defined to be proportional to d , as in the literature (Ilboudo et al., 2020), $\tilde{\nu}$ corresponds to the proportionality coefficient. With these, the gradients w.r.t. m , v , and ν

can be derived, respectively.

$$\begin{aligned}\nabla_m \ln \mathcal{T} &= -\frac{\nu + d - \nu^{-1}(g - m)v^{-1}}{2} \frac{1}{1 + \nu^{-1}dD} \\ &= \frac{\nu d^{-1} + 1}{\nu d^{-1} + D} \frac{g - m}{2v} \\ &= w_{mv} \frac{g - m}{2v} =: g_m\end{aligned}\quad (9)$$

$$\begin{aligned}\nabla_v \ln \mathcal{T} &= -\frac{1}{2v} - \frac{\nu + d - \nu^{-1}(g - m)^2 v^{-2}}{2} \frac{1}{1 + \nu^{-1}dD} \\ &= \frac{1}{2v^2} \left(\frac{\tilde{\nu} + 1}{\tilde{\nu} + D} s - v \right) \\ &= w_{mv} \frac{\tilde{\nu}\{(s - v) + (s - Dv)\tilde{\nu}^{-1}\}}{2v^2(\tilde{\nu} + 1)}\end{aligned}\quad (10)$$

$$\begin{aligned}\nabla_\nu \ln \mathcal{T} &= \frac{1}{2}\psi\left(\frac{\nu + d}{2}\right) - \frac{1}{2}\psi\left(\frac{\nu}{2}\right) - \frac{d}{2\nu} \\ &\quad - \frac{1}{2}\ln(1 + \nu^{-1}dD) - \frac{\nu + d}{2}\{(\nu + dD)^{-1} - \nu^{-1}\}\end{aligned}\quad (11)$$

where the gradients w.r.t. m and v are transformed so that the response to outliers can be intuitively analyzed by w_{mv} . ψ denotes the digamma function.

3.3. Modification of gradients

Since m is defined in the whole real space, gradient-based updates can be applied well. In contrast, for v and ν , their restricted domains require to modify the updates carefully.

For v , $(s - Dv)\tilde{\nu}^{-1}$ in eq. (10) would make the gradient-based update violate the domain of v , although its expectation would be zero since $\mathbb{E}[s] \rightarrow v$ and $\mathbb{E}[D] \rightarrow 1$. If v is larger than the exactly-estimated value, D and w_{mv} would become smaller and larger, respectively, namely the robustness to noise is impaired. However, since the Adam-like optimizers scale the update amounts by v , the effect of noise is expected to be insignificant. Therefore, we replace the relevant term by a simple upper bound as follows:

$$(s - Dv)\tilde{\nu}^{-1} \leq \max(\epsilon^2, (s - Dv)\tilde{\nu}^{-1}) =: \Delta s \quad (12)$$

where $\epsilon \ll 1$. With this modification, the surrogated gradient w.r.t. v is given by

$$\nabla_v \ln \mathcal{T} \leq w_{mv} \frac{\tilde{\nu}\{(s - v) + \Delta s\}}{2v^2(\tilde{\nu} + 1)} =: g_v \quad (13)$$

Compared to v , the gradient w.r.t. ν is more complex, and exactly when the domain of ν is violated cannot be identified. This is mainly due to the digamma function ψ , hence the first step is to use the upper and lower bounds of ψ to find the upper bound of the gradient w.r.t. ν . Note that the

use of an upper bound impairs the noise robustness, but as the maximum likelihood solution for ν has been reported to be overly robust, as described below, the following modification would not affect the learning performance so much.

Specifically, the upper and lower bounds of ψ is given as follows:

$$\ln x - \frac{1}{x} \leq \psi(x) \leq \ln x - \frac{1}{2x} \quad (14)$$

With these bounds, eq. (11) can be transformed to be the following upper bound.

$$\begin{aligned}\nabla_\nu \ln \mathcal{T} &\leq \frac{1}{2} \left\{ \ln(\nu + d) - \ln 2 - \frac{1}{\nu + d} - \ln \nu + \ln 2 + \frac{2}{\nu} \right. \\ &\quad \left. - \frac{d}{\nu} - \ln(\nu + dD) + \ln \nu - \frac{\nu + d}{\nu + dD} + 1 + \frac{d}{\nu} \right\} \\ &= \frac{1}{2} \left\{ -w_{mv} + \ln w_{mv} + 1 + \frac{\tilde{\nu} + 2}{\tilde{\nu} + 1\nu} \right\} \\ &= \frac{1}{2} \left\{ -w_{\tilde{\nu}} + 1 + \frac{\tilde{\nu} + 2}{\tilde{\nu} + 1\nu} \right\}\end{aligned}\quad (15)$$

where $w_{\tilde{\nu}} = w_{mv} - \ln w_{mv}$.

This overestimated gradient is very simple and its behavior is easy to understand. However, we found that its behavior is greatly affected by d , as shown in Fig. 1 with $\nu = d$. Note that it is not necessary to follow the literature (Ilboudo et al., 2020) for setting the degrees of freedom as $\nu = \tilde{\nu}d$, but this procedure is important to provide the same robustness to the respective subsets of parameters. In the case of $d = 1$, the gradient w.r.t. ν is negative only when w_{mv} is small enough to exclude noisy gradients w.r.t. parameters; otherwise, ν can be increased to suppress the robustness and make it easier to update the parameters. With $d \sim 10,000$ which is common for the weights matrix, it is unfortunately almost zero even when $w = 1$, and ν can only be decreased. Such a pessimistic behavior is consistent with the non-intuitive behavior of the multivariate student's t-distribution reported in the literature (Ley & Neven, 2012). This problem has also been empirically confirmed in (Ilboudo et al., 2021), where the robustness was forcibly suppressed by correcting the obtained (approximated) maximum likelihood estimate by multiplying it with d .

To alleviate this problem, we further consider an upper bound where ν is replaced by $\tilde{\nu}$ (or only the last term of eq. (15) is multiplied by $d \geq 1$). In addition, since ν does not appear directly in any gradients with this modification, it is more natural to deal with the gradient of $\tilde{\nu}$. The above

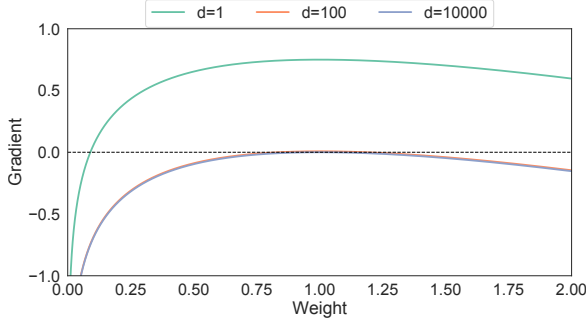


Figure 1. w_{mv} vs. the surrogated gradient in eq. (15) with $\nu = d$ according to several dimension sizes

modifications are finally summarized below.

$$\begin{aligned} \nabla_{\tilde{\nu}} \ln \mathcal{T} &= d \nabla_{\nu} \ln \mathcal{T} \\ &\leq \frac{d}{2} \left\{ -w_{\tilde{\nu}} + 1 + \frac{\tilde{\nu} + 2}{\tilde{\nu} + 1} \right\} \\ &= w_{\tilde{\nu}} \frac{d}{2} \left\{ -1 + \left(\frac{\tilde{\nu} + 2}{\tilde{\nu} + 1} + \tilde{\nu} \right) \frac{1}{\tilde{\nu} w_{\tilde{\nu}}} \right\} =: g_{\tilde{\nu}} \quad (16) \end{aligned}$$

As another interpretation, this upper bound is an approximation of the multivariate distribution by a univariate distribution. Although it is possible to model the distribution as a univariate distribution from the beginning of the derivation, there remains a concern that the robustness may be degraded since it captures the average without focusing on the amount of deviation in each axis.

3.4. Updates with adaptive step sizes

Now, we update the respective statistics, m , v , and $\tilde{\nu}$, by the gradient ascent with the obtained gradients in eqs. (9), (13), and (16). It is desired to comply with each domain and to use the same smoothness parameter as in the conventional Adam-like optimizers. To this end, we design the adaptive step sizes to convert the gradient ascent into the interpolation between the values before update and the update amounts (i.e. adaptive moving averages). Note, however, that the interpolation ratios obtained by appropriately designing the step sizes should be adaptive to outliers, namely, they should contain w_{mv} or $w_{\tilde{\nu}}$.

For m and v , the maximum value of w_{mv} can be easily found when $D \rightarrow 0$, i.e., $\bar{w}_{mv} = (\tilde{\nu} + 1)\tilde{\nu}^{-1}$. Therefore, the respective step sizes τ_m and τ_v are given as follows:

$$\tau_m = 2v \frac{1 - \beta}{\bar{w}_{mv}}, \quad \tau_v = 2v^2 \frac{\tilde{\nu} + 1}{\tilde{\nu}} \frac{1 - \beta}{\bar{w}_{mv}} \quad (17)$$

where $\beta \in (0, 1)$ corresponds to $\beta_{1,2}$ in Adam and others. With the notation $\tau_{mv} = (1 - \beta)w_{mv}\bar{w}_{mv}^{-1} \in (0, 1)$, m and

v can be updated using the above step sizes.

$$\begin{aligned} m_t &= m_{t-1} + \tau_m g_m \\ &= m_{t-1} + (1 - \beta)w_{mv}\bar{w}_{mv}^{-1}(g_t - m_{t-1}) \\ &= (1 - \tau_{mv})m_{t-1} + \tau_{mv}g_t \end{aligned} \quad (18)$$

$$\begin{aligned} v_t &= v_{t-1} + \tau_v g_v \\ &= v_{t-1} + (1 - \beta)w_{mv}\bar{w}_{mv}^{-1}(s + \Delta s - v_{t-1}) \\ &= (1 - \tau_{mv})v_{t-1} + \tau_{mv}(s + \Delta s) \end{aligned} \quad (19)$$

Since $\tau_{mv} \in (0, 1)$, it turns the update of v into an interpolation and $s + \Delta s \geq \epsilon^2$, $v \geq \epsilon^2$ is satisfied.

On the other hand, the implementation for $\tilde{\nu}$ is a bit tricky. We start by noticing that $w_{\tilde{\nu}}$ is a convex function over w_{mv} with a minimum value at $w_{mv} = 1$. The maximum value is therefore determined when w_{mv} is the largest or smallest. The maximum w_{mv} is already derived as \bar{w}_{mv} , but the minimum value cannot exactly be given since $w_{mv} \rightarrow 0$ when $D \rightarrow \infty$. Instead of the exact minimum value, we employ the float32 tiny value, which is the closest to zero numerically, resulting in $w_{\tilde{\nu}}(w_{mv} \simeq 0) \simeq 87.3365$. In summary, the maximum $w_{\tilde{\nu}}$, $\bar{w}_{\tilde{\nu}}$, can be defined as follows:

$$\bar{w}_{\tilde{\nu}} = \max(\bar{w}_{mv} - \ln(\bar{w}_{mv}), 87.3365) \quad (20)$$

If we design the step size with $\bar{w}_{\tilde{\nu}}$, we can obtain the update rule as interpolation of $\tilde{\nu}$ as well as m and v . However, although the minimum value of $\tilde{\nu}$ is expected to be positive, an excessive robustness inhibits the learning process. We therefore transform $\tilde{\nu} = \underline{\tilde{\nu}} + \Delta\tilde{\nu}$ with the user-specified minimum value, $\underline{\tilde{\nu}} > 0$, and the deviation, $\Delta\tilde{\nu} > 0$. With this transformation and the appropriate step size $\tau_{\Delta\tilde{\nu}}$ on gradient ascent for $\Delta\tilde{\nu}$, whose surrogated gradient is the same as eq. (16), the update rule of $\tilde{\nu}$ can be given as follows:

$$\tau_{\Delta\tilde{\nu}} = 2\Delta\tilde{\nu} \frac{1 - \beta}{d\bar{w}_{\tilde{\nu}}} \quad (21)$$

$$\begin{aligned} \Delta\tilde{\nu}_t &= \Delta\tilde{\nu}_{t-1} + \tau_{\Delta\tilde{\nu}} g_{\tilde{\nu}} \\ &= (1 - \tau_{\tilde{\nu}})\Delta\tilde{\nu}_{t-1} + \tau_{\tilde{\nu}} \left(\frac{\tilde{\nu}_{t-1} + 2}{\tilde{\nu}_{t-1} + 1} + \tilde{\nu}_{t-1} \right) \frac{\Delta\tilde{\nu}_{t-1}}{\tilde{\nu}_{t-1}w_{\tilde{\nu}}} \\ \tilde{\nu}_t &= (1 - \tau_{\tilde{\nu}})\tilde{\nu}_{t-1} + \tau_{\tilde{\nu}}\lambda \end{aligned} \quad (22)$$

where

$$\tau_{\tilde{\nu}} = (1 - \beta)w_{\tilde{\nu}}\bar{w}_{\tilde{\nu}}^{-1} \quad (23)$$

$$\lambda = \left(\frac{\tilde{\nu}_{t-1} + 2}{\tilde{\nu}_{t-1} + 1} + \tilde{\nu}_{t-1} \right) \frac{\tilde{\nu}_{t-1} - \underline{\tilde{\nu}}}{\tilde{\nu}_{t-1}w_{\tilde{\nu}}} + \underline{\tilde{\nu}} + \epsilon \quad (24)$$

Note that by adding $\underline{\tilde{\nu}} + \epsilon$ to both sides of the update rule for $\Delta\tilde{\nu}$, we get the update rule for $\tilde{\nu}$ directly.

Finally, the update amount of θ is given as follows:

$$\eta^{\text{AdaTerm}}(g_t) = \frac{m_t(1 - \beta^t)^{-1}}{\sqrt{v_t(1 - \beta^t)^{-1}}} \quad (25)$$

where, unlike Adam (Kingma & Ba, 2014), a small amount added to the denominator, ϵ , is removed since $\sqrt{v} \geq \epsilon$ in our implementation. Note that AdaBelief (Zhuang et al., 2020) also can remove it, although it is still added in the AdaBelief. Even though, the small amount in AdaBelief has little effect since the minimum of the scaling factor is, in comparison, absolutely larger.

3.5. Behavior analysis

First of all, as described in Appendix B, we have succeeded in obtaining the regret bound of AdaTerm. This analysis show that AdaTerm has the regret bound similar to that of conventional optimizers, if it is properly initialized under noise-free conditions. This means that AdaTerm can be used for any dataset without any concern, and can be used as a safety net easily.

The difference from the related work (Ilboudo et al., 2020) is the way of interpolating between the value before the update and the update amount. In the past work, the discounted sum of w_{mv} was used, but in AdaTerm, \bar{w}_{mv} is used, which eliminates the need to store the discounted sum in memory. Despite that, since w_{mv} is still used to determine whether or not to exclude aberrant updates, the essential behavior is expected to be kept.

Secondly, v is now updated robustly depending on w_{mv} , that would not loosen the threshold for aberrant update amounts in the next and subsequent steps even when the aberrant update amounts are given. In addition, it is expected to coordinate among the axes. That is, if an anomaly is detected only on a particular axis, Δs on that axis will become larger, making v on that axis larger and mitigating the anomaly detection. Conversely, if anomalies are detected in most axes, $\Delta s \simeq \epsilon^2$ will continue to exclude the anomalies as described above. Such adaptive behaviors would yield stable updates even if β is smaller than the conventional β_2 ($= 0.999$ in most optimizers).

Thirdly, the robustness indicator \tilde{v} will be increased when $w_{mv} \simeq 1$ without noise, in which case $w_{\tilde{v}} \simeq 1$ and the first term of λ becomes larger. However, the increase speed is limited by $\bar{w}_{\tilde{v}}$. On the other hand, if an aberrant value is given, $w_{\tilde{v}} \gg 1$, it will decay towards $\underline{\tilde{v}}$ more quickly than the increase speed. Thus, although the robustness tuning mechanism substitutes the upper bound of its gradient, it still behaves conservatively and can be expected to retain its excellent robustness to noise.

Finally, if $\underline{\tilde{v}} \rightarrow \infty$, the robustness is lost and AdaTerm essentially matches AdaBelief, although there is a possible performance difference due to the simplification of the hyper-parameters. Therefore, in problems where AdaBelief would be effective, AdaTerm would perform well as well.

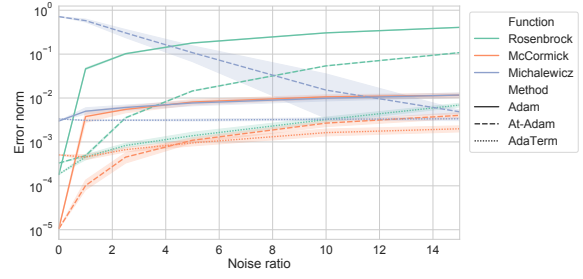


Figure 2. Noise ratio vs. L2 norm between the converged point and the analytically-optimal point

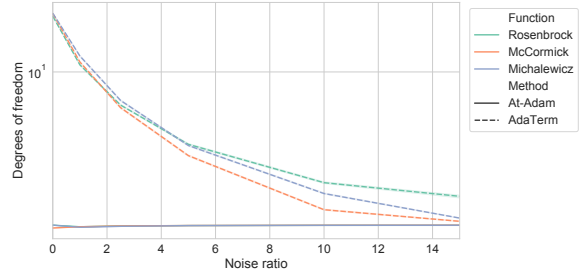


Figure 3. Noise ratio vs. degrees of freedom ν

4. Experiments

4.1. Analysis with test functions

Before solving more practical benchmark problems, we analyze the behavior of AdaTerm through minimization of typical test functions. In other words, we aim to find the two-dimensional point where the respective potential fields is minimized by relying on the gradients of the potential fields. To analyze the robustness to noise, uniformly distributed noise ($\in (-0.1, 0.1)$) at a specified ratio is added to the point coordinates to be optimized.

The results are summarized in Figs. 2 and 3 (details are in Appendix C). Fig. 2, which shows the error norm from the analytically-optimal point, shows that the convergence accuracy of McCormick function with AdaTerm was not good in lower noise ratio probably due to large learning rate. In other scenes, however, AdaTerm was able to maintain its normal update performance while mitigating the effect of noise. The performance of Adam (Kingma & Ba, 2014) was significantly degraded when some noise is given, indicating the sensitivity to noise. On Michalewicz function with At-Adam (Ilboudo et al., 2021), the steep gradients toward the optimal value would be judged as noise and excluded, and the optimal solution was not obtained. This result implies that At-Adam has insufficient adaptability of robustness to noise by automatically tuning ν . Indeed, Fig. 3, which plots the final ν , shows that ν with At-Adam converged to a

nearly constant value independent of noise. In contrast, ν of AdaTerm was inversely proportional to the noise ratio, and succeeded in achieving an intuitively natural behavior of increasing ν when the noise is rare, and decreasing ν when the noise is often mixed.

4.2. Configurations of benchmark problems

We perform four benchmark problems to compare the performance of typical optimizers, including the proposed AdaTerm. Detailed setups (e.g. network architectures) can be found in Appendix D.

4.2.1. CLASSIFICATION OF MISLABELED CIFAR-100

The first problem is an image classification problem with CIFAR-100 dataset. As artificial noise, some proportion of the labels (0 % and 10 %) on the training data is randomized to be anything other than the true labels. As a simple data augmentation, random horizontal flip is introduced along with 4 padding only when training.

Its loss function is given to be the cross-entropy. In order to stabilize the learning performance, we introduce a label smoothing technique (Szegedy et al., 2016). The degree of smoothing is set to 20%, referring to the literature (Lukasik et al., 2020).

4.2.2. LONG-TERM PREDICTION OF ROBOT LOCOMOTION

The second problem is a motion prediction problem. The dataset used was made in the literature (Kobayashi, 2020), which contains training data for 150 trajectories, validation data for 25 trajectories, and test data for 25 trajectories of a hexapod locomotion with 18 observed joint angles and 18 reference joint angles. An agent continues to predict the states within the given time interval (1 and 30 steps) from the initial true state and subsequent predicted states. Therefore, the predicted states used as inputs would deviate from the true ones and become noise for learning.

For the loss function, instead of the mean squared error (MSE), which is commonly used, we employ the negative log likelihood (NLL) of the predictive distribution, which allows the scale difference of each state to be considered internally. NLL is computed at each prediction step, then their sum is used as the loss function. Because of the high cost of back-propagation through time (BPTT) over the entire trajectory, truncated BPTT (30 steps on average) (Puskorius & Feldkamp, 1994; Tallec & Ollivier, 2017) is introduced.

4.2.3. REINFORCEMENT LEARNING ON PYBULLET SIMULATOR

The third problem is RL simulated by Pybullet engine with OpenAI Gym (Brockman et al., 2016; Coumans & Bai,

2016). The tasks to be solved are Hopper and Ant, both of which require an agent to move as straight as possible on flat terrain. As mentioned before, RL relies on estimated values due to no true signals, which can easily introduce noise in the training.

The RL algorithm implemented is an actor-critic algorithm based on the literature (Kobayashi, 2021). The agent only learns after each episode using experience replay. This experience replay samples 128 batches after each episode, and its buffer size is set to be small enough (i.e. 10,000) to reveal the influence of noise.

4.2.4. POLICY DISTILLATION BY BEHAVIORAL CLONING

The fourth problem is the policy distillation (Rusu et al., 2015). The three policies for Ant that were properly learned in the RL problem above were taken as experts, and 10 trajectories of state-action pairs were collected from each of them. We also collected three trajectories from the one policy that fell into a local solution as an amateur. In the dataset constructed with these trajectories, not only the amateur trajectories, but also the expert trajectories would not be always truly optimal, and thus they cause noise.

The loss function is the negative log likelihood of the policy according to behavioral cloning (Bain & Sammut, 1995), which is the simplest way of imitation learning. In addition, a weight decay is added to prevent the small networks (i.e. the distillation target) from fitting particular behaviors.

4.3. Results of benchmark problems

In all the experiments, we compare the following six optimizers: Adam (Kingma & Ba, 2014), AdaBelief (Zhuang et al., 2020), and RAdam (Gulcehre et al., 2017) as the state-of-the-art optimizers in the cases without noise; t-Adam (Ilboudo et al., 2020) and At-Adam (Ilboudo et al., 2021) as the noise-robust optimizers; and AdaTerm as our proposal. Note that the initial ν in At-Adam is set to be the same value of t-Adam to evaluate its adaptiveness. In each condition, 24 trials are conducted with different random seeds, and the mean and standard deviation of the scores for the respective benchmarks are evaluated. All the test results after learning can be found in Table 1. The ablation test was also conducted, as summarized in Appendix E.

Since we prepared benchmarks that favor noise-robust optimizers, AdaTerm obtained the best in most of the problems (except for 1-step prediction and Ant task in RL). Since 1-step prediction is a relatively simple supervised learning, it does not need robustness to noise. Therefore, as like the error norm of McCormick function in Fig. 2, the too high learning rate caused by $\beta < \beta_2$ contributed to the performance degradation. Although AdaTerm for Ant task in RL was certainly not the best score, we can confirm its

Table 1. Experimental results: the best in all the results for each benchmark is written in bold; the numbers in parentheses denote standard deviations.

Method	Classification		Prediction		RL		Distillation	
	Accuracy		MSE at final prediction		The sum of rewards		The sum of rewards	
	0 %	10 %	1 step	30 steps	Hopper	Ant	w/o amateur	w/ amateur
Adam	0.721	0.681	0.032	1.243	1338	860	1657	1432
	(4.3e-3)	(4.9e-3)	(3.9e-4)	(1.4e-1)	(6.9e+2)	(3.8e+2)	(2.9e+2)	(2.1e+2)
AdaBelief	0.723	0.680	0.032	1.177	1382	864	1673	1395
	(5.6e-3)	(3.9e-3)	(4.8e-4)	(9.4e-2)	(6.9e+2)	(4.3e+2)	(2.2e+2)	(2.7e+2)
RAdam	0.719	0.680	0.033	1.096	1489	894	1625	1326
	(4.3e-3)	(3.4e-3)	(3.7e-4)	(1.5e-1)	(5.5e+2)	(4.0e+2)	(2.2e+2)	(2.4e+2)
t-Adam	0.717	0.680	0.032	1.022	1356	2222	1647	1333
	(5.7e-3)	(3.1e-3)	(4.2e-4)	(2.1e-1)	(7.0e+2)	(2.7e+2)	(1.9e+2)	(1.8e+2)
At-Adam	0.718	0.681	0.032	1.111	1568	2191	1683	1395
	(4.2e-3)	(4.0e-3)	(3.6e-4)	(2.0e-1)	(5.3e+2)	(3.4e+2)	(1.9e+2)	(2.2e+2)
AdaTerm	0.731	0.682	0.034	0.907	1705	1986	1737	1528
(Ours)	(3.7e-3)	(4.5e-3)	(5.6e-4)	(1.4e-1)	(6.3e+2)	(3.8e+2)	(2.0e+2)	(1.6e+2)

usefulness from the fact that Ant task was only successful with noise-robust optimizers. In summary, we can say that AdaTerm can maintain its learning performance better than other optimizers in practical problems with noise.

We analyze the remarkable results of the benchmark problems, respectively. In the classification problem, AdaTerm achieved the highest classification performance in the compared optimizers even for the 0% label error. This is because CIFAR-100 contains general images, which are prone to be with noise, and the training dataset has only 500 images per class, revealing the adverse effects of noise.

In the 30-step prediction, AdaTerm was the only one that succeeded in making MSE below 1. We can easily expect that this problem is noise-contained due to inaccurate estimated inputs. However, as learning progresses, the accuracy of the estimated inputs should be improved, and the noise robustness would gradually become unnecessary. In AdaTerm, the adjustment of the noise robustness worked properly (like Fig. 3), and was successful in accelerating learning.

In the RL problem, as mentioned before, it is clear that Ant task required the high robustness to noise. In addition, as one of the implementation tips in RL, it is often pointed out that setting a relatively large ϵ contributes to the stability of learning. AdaTerm has larger ϵ (i.e. $1e-5$) as the default value for the enough minimal adjustment speed of \tilde{v} , which may also contribute to the performance improvement.

Finally, in the policy distillation, the performance improvement by AdaTerm was confirmed even when amateur data, which is a source of noise, was not included. This is due to the difficulty to express the same behaviors with limited resources, and some redundant or unnecessary behaviors need to be eliminated. Such behaviors would be regarded

as noise since their ratio is smaller than one of the normal behaviors, hence AdaTerm succeeded in excluding them and distilling the normal behaviors.

5. Conclusion

We presented the AdaTerm optimizer, which is adaptively robust to noise and outliers, for deep learning. AdaTerm was derived from the assumption that the gradients are generated from multivariate diagonal student's t-distribution, and then, its sample statistics are optimized through the surrogated maximum log-likelihood estimation. Optimization of test functions revealed that AdaTerm can adjust its robustness to noise in accordance with the impact of the noise. Through the four typical benchmarks, we confirmed that the robustness to noise and the learning performance of AdaTerm are as good as or better than those of conventional optimizers.

This paper focused on computing statistics amounts, but in recent years, the importance of integration with raw SGD (i.e., decay of scaling in Adam-like optimizers) has been confirmed (Luo et al., 2019; Zhou et al., 2020). Similar functions can be expected in AdaTerm by reviewing Δs , hence we will develop a new version in the near future. In addition, following AdaBelief, AdaTerm normalizes the gradients (more precisely, its first momentum) by scale instead of second momentum, although there is no discussion on which one is more effective. Therefore, We will pursue the theory of this point, and introduce a mechanism to adaptively switch the use of both when there are pros/cons.

References

Aeschliman, C., Park, J., and Kak, A. C. A novel parameter estimation algorithm for the multivariate t-distribution

- and its application to computer vision. In *European conference on computer vision*, pp. 594–607. Springer, 2010.
- Alacaoglu, A., Malitsky, Y., Mertikopoulos, P., and Cevher, V. A new regret analysis for adam-type algorithms. In *International Conference on Machine Learning*, pp. 202–210. PMLR, 2020.
- Ba, J. L., Kiros, J. R., and Hinton, G. E. Layer normalization. *arXiv preprint arXiv:1607.06450*, 2016.
- Bain, M. and Sammut, C. A framework for behavioural cloning. In *Machine Intelligence 15*, pp. 103–129, 1995.
- Brockman, G., Cheung, V., Pettersson, L., Schneider, J., Schulman, J., Tang, J., and Zaremba, W. Openai gym. *arXiv preprint arXiv:1606.01540*, 2016.
- Chen, R. T., Rubanova, Y., Bettencourt, J., and Duvenaud, D. Neural ordinary differential equations. In *International Conference on Neural Information Processing Systems*, pp. 6572–6583, 2018.
- Chung, J., Gulcehre, C., Cho, K., and Bengio, Y. Empirical evaluation of gated recurrent neural networks on sequence modeling. *arXiv preprint arXiv:1412.3555*, 2014.
- Coumans, E. and Bai, Y. Pybullet, a python module for physics simulation for games, robotics and machine learning. *GitHub repository*, 2016.
- De Ryck, T., Lanthaler, S., and Mishra, S. On the approximation of functions by tanh neural networks. *Neural Networks*, 143:732–750, 2021.
- Doğru, F. Z., Bulut, Y. M., and Arslan, O. Doubly reweighted estimators for the parameters of the multivariate t-distribution. *Communications in Statistics-Theory and Methods*, 47(19):4751–4771, 2018.
- Elfwing, S., Uchibe, E., and Doya, K. Sigmoid-weighted linear units for neural network function approximation in reinforcement learning. *Neural Networks*, 107:3–11, 2018.
- Gou, J., Yu, B., Maybank, S. J., and Tao, D. Knowledge distillation: A survey. *International Journal of Computer Vision*, 129(6):1789–1819, 2021.
- Gulcehre, C., Sotelo, J., Moczulski, M., and Bengio, Y. A robust adaptive stochastic gradient method for deep learning. In *International Joint Conference on Neural Networks*, pp. 125–132. IEEE, 2017.
- He, K., Zhang, X., Ren, S., and Sun, J. Deep residual learning for image recognition. In *IEEE conference on computer vision and pattern recognition*, pp. 770–778, 2016.
- Holland, M. J. and Ikeda, K. Efficient learning with robust gradient descent. *Machine Learning*, 108(8):1523–1560, 2019.
- Ilboudo, W. E. L., Kobayashi, T., and Sugimoto, K. Robust stochastic gradient descent with student-t distribution based first-order momentum. *IEEE Transactions on Neural Networks and Learning Systems*, 2020.
- Ilboudo, W. E. L., Kobayashi, T., and Sugimoto, K. Adaptive t-momentum-based optimization for unknown ratio of outliers in amateur data in imitation learning. In *IEEE/RSJ International Conference on Intelligent Robots and Systems*, pp. 7851–7857. IEEE, 2021.
- Kim, K.-S. and Choi, Y.-S. Hyadamc: A new adam-based hybrid optimization algorithm for convolution neural networks. *Sensors*, 21(12):4054, 2021.
- Kingma, D. P. and Ba, J. Adam: A method for stochastic optimization. *arXiv preprint arXiv:1412.6980*, 2014.
- Kishida, M., Ogura, M., Yoshida, Y., and Wadayama, T. Deep learning-based average consensus. *IEEE Access*, 8: 142404–142412, 2020.
- Kobayashi, T. Student-t policy in reinforcement learning to acquire global optimum of robot control. *Applied Intelligence*, 49(12):4335–4347, 2019.
- Kobayashi, T. q-vae for disentangled representation learning and latent dynamical systems. *IEEE Robotics and Automation Letters*, 5(4):5669–5676, 2020.
- Kobayashi, T. Proximal policy optimization with relative pearson divergence. In *2021 IEEE International Conference on Robotics and Automation (ICRA)*, pp. 8416–8421. IEEE, 2021.
- Lange, K. L., Little, R. J., and Taylor, J. M. Robust statistical modeling using the t distribution. *Journal of the American Statistical Association*, 84(408):881–896, 1989.
- LeCun, Y., Bengio, Y., and Hinton, G. Deep learning. *nature*, 521(7553):436, 2015.
- Ley, C. and Neven, A. The value at the mode in multivariate t distributions: a curiosity or not? *arXiv preprint arXiv:1211.1174*, 2012.
- Liu, L., Jiang, H., He, P., Chen, W., Liu, X., Gao, J., and Han, J. On the variance of the adaptive learning rate and beyond. In *International Conference on Learning Representations*, 2020.
- Lukasik, M., Bhojanapalli, S., Menon, A., and Kumar, S. Does label smoothing mitigate label noise? In *International Conference on Machine Learning*, pp. 6448–6458. PMLR, 2020.

- Luo, L., Xiong, Y., Liu, Y., and Sun, X. Adaptive gradient methods with dynamic bound of learning rate. In *International Conference on Learning Representations*, 2019.
- Ma, X., Huang, H., Wang, Y., Romano, S., Erfani, S., and Bailey, J. Normalized loss functions for deep learning with noisy labels. In *International Conference on Machine Learning*, pp. 6543–6553. PMLR, 2020.
- Mirylenka, K., Giannakopoulos, G., Do, L., and Palpanas, T. On classifier behavior in the presence of mislabeling noise. *Data Mining & Knowledge Discovery*, 31(3), 2017.
- Paszke, A., Gross, S., Chintala, S., Chanan, G., Yang, E., DeVito, Z., Lin, Z., Desmaison, A., Antiga, L., and Lerer, A. Automatic differentiation in pytorch. In *Advances in Neural Information Processing Systems Workshop*, 2017.
- Prasad, A., Suggala, A. S., Balakrishnan, S., and Ravikumar, P. Robust estimation via robust gradient estimation. *Journal of the Royal Statistical Society: Series B (Statistical Methodology)*, 82(3):601–627, 2020.
- Puskorius, G. and Feldkamp, L. Truncated backpropagation through time and kalman filter training for neurocontrol. In *IEEE International Conference on Neural Networks*, volume 4, pp. 2488–2493. IEEE, 1994.
- Reddi, S. J., Kale, S., and Kumar, S. On the convergence of adam and beyond. In *International Conference on Learning Representations*, 2018.
- Robbins, H. and Monro, S. A stochastic approximation method. *The annals of mathematical statistics*, pp. 400–407, 1951.
- Rusu, A. A., Colmenarejo, S. G., Gulcehre, C., Desjardins, G., Kirkpatrick, J., Pascanu, R., Mnih, V., Kavukcuoglu, K., and Hadsell, R. Policy distillation. *arXiv preprint arXiv:1511.06295*, 2015.
- Schmidt, R. M., Schneider, F., and Hennig, P. Descending through a crowded valley-benchmarking deep learning optimizers. In *International Conference on Machine Learning*, pp. 9367–9376. PMLR, 2021.
- Simsekli, U., Sagun, L., and Gurbuzbalaban, M. A tail-index analysis of stochastic gradient noise in deep neural networks. In *International Conference on Machine Learning*, pp. 5827–5837. PMLR, 2019.
- Suchi, M., Patten, T., Fischinger, D., and Vincze, M. Easylabel: a semi-automatic pixel-wise object annotation tool for creating robotic rgb-d datasets. In *International Conference on Robotics and Automation*, pp. 6678–6684. IEEE, 2019.
- Sun, S., Cao, Z., Zhu, H., and Zhao, J. A survey of optimization methods from a machine learning perspective. *IEEE transactions on cybernetics*, 50(8):3668–3681, 2019.
- Sutton, R. S. and Barto, A. G. *Reinforcement learning: An introduction*. MIT press, 2018.
- Szegedy, C., Vanhoucke, V., Ioffe, S., Shlens, J., and Wojna, Z. Rethinking the inception architecture for computer vision. In *IEEE conference on computer vision and pattern recognition*, pp. 2818–2826, 2016.
- Tallec, C. and Ollivier, Y. Unbiasing truncated backpropagation through time. *arXiv preprint arXiv:1705.08209*, 2017.
- Xu, J., Sun, X., Zhang, Z., Zhao, G., and Lin, J. Understanding and improving layer normalization. *Advances in Neural Information Processing Systems*, 32:4381–4391, 2019.
- Zhou, P., Feng, J., Ma, C., Xiong, C., Hoi, S. C. H., et al. Towards theoretically understanding why sgd generalizes better than adam in deep learning. *Advances in Neural Information Processing Systems*, 33, 2020.
- Zhuang, J., Tang, T., Ding, Y., Tatikonda, S. C., Dvornek, N., Papademetris, X., and Duncan, J. Adabelief optimizer: Adapting stepsizes by the belief in observed gradients. *Advances in Neural Information Processing Systems*, 33, 2020.

Algorithm 1 AdaTerm optimizer

```

1: Set  $\alpha > 0$  ( $10^{-3}$  is the default value)
2: Set  $\beta \in (0, 1)$  (0.9 is the default value)
3: Set  $\epsilon \ll 1$  ( $10^{-5}$  is the default value)
4: Set  $\underline{\tilde{\nu}} > 0$  (1 is the default value)
5: Set  $d$  as the dimension size of each subset of parameters
6: Initialize  $\tilde{D}, \theta_0, m_0 \leftarrow 0, v_0 \leftarrow \epsilon^2, \tilde{\nu}_0 \leftarrow \underline{\tilde{\nu}} + \epsilon, t \leftarrow 0$ 
7: while  $\theta_t$  not converged do
8:   // Compute gradient
9:    $t \leftarrow t + 1$ 
10:   $g_t = \nabla_{\theta_{t-1}} \mathcal{L}_{\mathcal{B}_t}, \mathcal{B}_t \sim \tilde{D}$ 
11:  // Compute index of outlier
12:   $s = (g_t - m_{t-1})^2$ 
13:   $D = d^{-1} s^\top v_{t-1}^{-1}$ 
14:  // Compute adaptive step sizes
15:   $w_{mv} = (\tilde{\nu}_{t-1} + 1)(\tilde{\nu}_{t-1} + D)^{-1}$ 
16:   $\bar{w}_{mv} = (\tilde{\nu}_{t-1} + 1)\tilde{\nu}_{t-1}^{-1}$ 
17:   $w_{\tilde{\nu}} = w_{mv} - \ln(w_{mv})$ 
18:   $\bar{w}_{\tilde{\nu}} = \max(\bar{w}_{mv} - \ln(\bar{w}_{mv}), 87.3365)$ 
19:   $\tau_{mv} = (1 - \beta) \frac{w_{mv}}{\bar{w}_{mv}}, \tau_{\tilde{\nu}} = (1 - \beta) \frac{w_{\tilde{\nu}}}{\bar{w}_{\tilde{\nu}}}$ 
20:  // Compute update amounts
21:   $\Delta s = \max(\epsilon^2, (s - Dv_{t-1})\tilde{\nu}_{t-1}^{-1})$ 
22:   $\lambda = \left( \frac{\tilde{\nu}_{t-1} + 2}{\tilde{\nu}_{t-1} + 1} + \tilde{\nu}_{t-1} \right) \frac{\tilde{\nu}_{t-1} - \underline{\tilde{\nu}}}{\tilde{\nu}_{t-1} w_{\tilde{\nu}}} + \underline{\tilde{\nu}} + \epsilon$ 
23:  // Update parameters
24:   $m_t = (1 - \tau_{mv})m_{t-1} + \tau_{mv}g_t$ 
25:   $v_t = (1 - \tau_{mv})v_{t-1} + \tau_{mv}(s + \Delta s)$ 
26:   $\tilde{\nu}_t = (1 - \tau_{\tilde{\nu}})\tilde{\nu}_{t-1} + \tau_{\tilde{\nu}}\lambda$ 
27:   $\theta_t = \theta_{t-1} - \alpha \frac{m_t(1 - \beta^t)^{-1}}{\sqrt{v_t(1 - \beta^t)^{-1}}}$ 
28: end while

```

A. Pseudocode

The pseudocode of AdaTerm is described in Alg. 1. Here, $\beta \in (0, 1)$ denotes the common smoothness parameter (i.e. $\beta = \beta_1 = \beta_2$ in the other optimizers), $\epsilon \ll 1$ stabilizes computation, and $\underline{\tilde{\nu}}$ is for controlling excessive robustness. The real value 87.3365 in $\bar{w}_{\tilde{\nu}}$ is given when w_{mv} is the tiny value (i.e. closest to zero) on float32. The minimum value of $\Delta\tilde{\nu} = \tilde{\nu} - \underline{\tilde{\nu}}$ is given by ϵ so that $\Delta\tilde{\nu} > 0$ is satisfied. This process also prevents the first term of λ from becoming 0 and stopping the update of $\tilde{\nu}$.

B. Proof of regret bound

B.1. Preliminaries

$$\tau_t = (1 - \beta) \frac{\nu_{t-1}}{\nu_{t-1} + 1} \frac{d\nu_{t-1} + d}{d\nu_{t-1} + \|g_t - m_{t-1}\|_{v_{t-1}^{-1}}^2} = (1 - \beta) \frac{d\nu_{t-1}}{d\nu_{t-1} + \|g_t - m_{t-1}\|_{v_{t-1}^{-1}}^2}$$

with $\|g_t\|_\infty \leq G_\infty$, then we also have $\|g_t - m_{t-1}\|_\infty \leq 2G_\infty$. Therefore,

$$\|g_t - m_{t-1}\|_{v_{t-1}^{-1}}^2 = \sum_{i=1}^d v_{t-1,i}^{-1} (g_{t,i} - m_{t-1,i})^2 \leq \sum_{i=1}^d \epsilon^{-2} (2G_\infty)^2 = 4d\epsilon^{-2} G_\infty^2$$

Furthermore, for $A \geq 1$,

$$\frac{d\tilde{\nu}_c}{d\tilde{\nu}_c + A} \leq \frac{d\nu_{t-1}}{d\nu_{t-1} + A} \leq 1$$

where $\tilde{\nu}_c \geq \underline{\nu}$. From $t = 1$ to $t = \hat{T} \leq T$, $\tilde{\nu}_c$ should be $\underline{\nu}$ as the non-convergent period. Afterwards, we can set $\tilde{\nu}_c$ to be more specific convergent value (see later).

From the definition of τ_t , we see that (assuming $4d\epsilon^{-2}G_\infty^2 \geq 1$, which should normally be true):

$$\frac{d(1 - \beta)\tilde{\nu}_c}{d\tilde{\nu}_c + 4d\epsilon^{-2}G_\infty^2} \leq \tau_t \leq (1 - \beta) \quad (26)$$

From which we can derive the two following relations:

$$\beta \leq (1 - \tau_t) \leq \frac{d\beta\tilde{\nu}_c + 4d\epsilon^{-2}G_\infty^2}{d\tilde{\nu}_c + 4d\epsilon^{-2}G_\infty^2} \quad (27)$$

$$\frac{\beta}{1 - \beta} \leq \frac{1 - \tau_t}{\tau_t} \leq \frac{d\beta\tilde{\nu}_c + 4d\epsilon^{-2}G_\infty^2}{d\tilde{\nu}_c} \quad (28)$$

B.2. Convex Optimization

Let m_t and v_t be the momentum and variance produced by AdaTerm, then:

$$m_t = (1 - \tau_t)m_{t-1} + \tau_t g_t, \quad v_t = (1 - \tau_t)m_{t-1} + \tau_t ((g_t - m_{t-1})^2 + \Delta s) \quad (29)$$

We therefore have:

$$g_t = \frac{1}{\tau_t} m_t - \frac{1 - \tau_t}{\tau_t} m_{t-1} \quad (30)$$

which leads to:

$$\langle g_t, x_t - x \rangle = \frac{1}{\tau_t} \langle m_t, x_t - x \rangle - \frac{1 - \tau_t}{\tau_t} \langle m_{t-1}, x_t - x \rangle \quad (31)$$

$$= \frac{1}{\tau_t} \langle m_t, x_t - x \rangle - \frac{1 - \tau_t}{\tau_t} \langle m_{t-1}, x_{t-1} - x \rangle - \frac{1 - \tau_t}{\tau_t} \langle m_{t-1}, x_t - x_{t-1} \rangle \quad (32)$$

$$= \frac{1}{\tau_t} (\langle m_t, x_t - x \rangle - \langle m_{t-1}, x_{t-1} - x \rangle) + \langle m_{t-1}, x_{t-1} - x \rangle - \frac{1 - \tau_t}{\tau_t} \langle m_{t-1}, x_t - x_{t-1} \rangle \quad (33)$$

We therefore have that:

$$\sum_{t=1}^T \langle g_t, x_t - x \rangle = R_{1,t} + R_{2,t} + R_{3,t} \quad (34)$$

$$R_{1,t} = \sum_{t=1}^T \langle m_{t-1}, x_{t-1} - x \rangle \quad (35)$$

$$R_{2,t} = - \sum_{t=1}^T \frac{1 - \tau_t}{\tau_t} \langle m_{t-1}, x_t - x_{t-1} \rangle \quad (36)$$

$$R_{3,t} = \sum_{t=1}^T \frac{1}{\tau_t} (\langle m_t, x_t - x \rangle - \langle m_{t-1}, x_{t-1} - x \rangle) \quad (37)$$

B.2.1. BOUND OF $R_{1,t}$

$$\sum_{t=1}^T \langle m_{t-1}, x_{t-1} - x \rangle = \sum_{k=0}^{T-1} \langle m_k, x_k - x \rangle = \langle m_0, x_0 - x \rangle + \sum_{k=1}^{T-1} \langle m_k, x_k - x \rangle = \sum_{t=1}^{T-1} \langle m_t, x_t - x \rangle$$

With the projection operator, i.e. $x_{t+1} = \Pi_{\chi, \hat{v}_t^{1/2}}(x_t - \alpha_t \hat{v}_t^{-1/2} m_t) = \arg \min_{x \in \chi} \|x - (x_t - \alpha_t \hat{v}_t^{-1/2} m_t)\|_{\hat{v}_t^{1/2}}$ and its non-expansive property, we have that (given that $x \in \chi$, i.e. $\Pi_{\chi, \hat{v}_t^{1/2}}(x) = x$):

$$\begin{aligned} \|x_{t+1} - x\|_{\hat{v}_t^{1/2}}^2 &= \left\| \Pi_{\chi, \hat{v}_t^{1/2}}(x_t - \alpha_t \hat{v}_t^{-1/2} m_t) - \Pi_{\chi, \hat{v}_t^{1/2}}(x) \right\|_{\hat{v}_t^{1/2}}^2 \\ &\leq \left\| (x_t - \alpha_t \hat{v}_t^{-1/2} m_t) - x \right\|_{\hat{v}_t^{1/2}}^2 = \|x_t - x\|_{\hat{v}_t^{1/2}}^2 - 2\alpha_t \langle m_t, x_t - x \rangle + \left\| \alpha_t \hat{v}_t^{-1/2} m_t \right\|_{\hat{v}_t^{1/2}}^2 \end{aligned}$$

Which implies:

$$\langle m_t, x_t - x \rangle \leq \frac{1}{2\alpha_t} \|x_t - x\|_{\hat{v}_t^{1/2}}^2 - \frac{1}{2\alpha_t} \|x_{t+1} - x\|_{\hat{v}_t^{1/2}}^2 + \frac{\alpha_t}{2} \left\| \hat{v}_t^{-1/2} m_t \right\|_{\hat{v}_t^{1/2}}^2 \quad (38)$$

$$\begin{aligned} &= \frac{1}{2\alpha_t} \|x_t - x\|_{\hat{v}_t^{1/2}}^2 - \frac{1}{2\alpha_t} \|x_{t+1} - x\|_{\hat{v}_t^{1/2}}^2 + \frac{\alpha_t}{2} \left\| \hat{v}_t^{-1/2} m_t \right\|_{\hat{v}_t^{1/2}}^2 \\ &\quad + \frac{1}{2\alpha_{t-1}} \|x_t - x\|_{\hat{v}_{t-1}^{1/2}}^2 - \frac{1}{2\alpha_{t-1}} \|x_t - x\|_{\hat{v}_{t-1}^{1/2}}^2 \\ &= \frac{1}{2\alpha_{t-1}} \|x_t - x\|_{\hat{v}_{t-1}^{1/2}}^2 - \frac{1}{2\alpha_t} \|x_{t+1} - x\|_{\hat{v}_t^{1/2}}^2 + \frac{\alpha_t}{2} \left\| \hat{v}_t^{-1/2} m_t \right\|_{\hat{v}_t^{1/2}}^2 \\ &\quad + \frac{1}{2\alpha_t} \|x_t - x\|_{\hat{v}_t^{1/2}}^2 - \frac{1}{2\alpha_{t-1}} \|x_t - x\|_{\hat{v}_{t-1}^{1/2}}^2 \\ &= \frac{1}{2\alpha_{t-1}} \|x_t - x\|_{\hat{v}_{t-1}^{1/2}}^2 - \frac{1}{2\alpha_t} \|x_{t+1} - x\|_{\hat{v}_t^{1/2}}^2 + \frac{\alpha_t}{2} \left\| \hat{v}_t^{-1/2} m_t \right\|_{\hat{v}_t^{1/2}}^2 \\ &\quad + \frac{1}{2} \sum_{i=1}^d \left(\frac{\hat{v}_{t,i}^{1/2}}{\alpha_t} - \frac{\hat{v}_{t-1,i}^{1/2}}{\alpha_{t-1}} \right) (x_{t,i} - x_i)^2 \end{aligned} \quad (39)$$

$$\begin{aligned} &\leq \frac{1}{2\alpha_{t-1}} \|x_t - x\|_{\hat{v}_{t-1}^{1/2}}^2 - \frac{1}{2\alpha_t} \|x_{t+1} - x\|_{\hat{v}_t^{1/2}}^2 + \frac{\alpha_t}{2} \left\| \hat{v}_t^{-1/2} m_t \right\|_{\hat{v}_t^{1/2}}^2 \\ &\quad + \frac{D_\infty^2}{2} \sum_{i=1}^d \left(\frac{\hat{v}_{t,i}^{1/2}}{\alpha_t} - \frac{\hat{v}_{t-1,i}^{1/2}}{\alpha_{t-1}} \right) \end{aligned} \quad (40)$$

Where the last inequality is due to $\|x_t - x\|_\infty \leq D_\infty$ and $\frac{\hat{v}_{t,i}^{1/2}}{\alpha_t} \geq \frac{\hat{v}_{t-1,i}^{1/2}}{\alpha_{t-1}}$. Now, summing over $t = 1, \dots, T-1$ and simplifying the telescoping sums, we get:

$$\begin{aligned}
 \sum_{t=1}^{T-1} \langle m_t, x_t - x \rangle &\leq \frac{1}{2\alpha_0} \|x_1 - x\|_{\hat{v}_0^{1/2}}^2 - \frac{1}{2\alpha_{T-1}} \|x_T - x\|_{\hat{v}_{T-1}^{1/2}}^2 + \sum_{t=1}^{T-1} \frac{\alpha_t}{2} \left\| \hat{v}_t^{-1/2} m_t \right\|_{\hat{v}_t^{1/2}}^2 \\
 &\quad + \frac{D_\infty^2}{2} \sum_{i=1}^d \left(\frac{\hat{v}_{T-1,i}^{1/2}}{\alpha_{T-1}} - \frac{\hat{v}_{0,i}^{1/2}}{\alpha_0} \right) \\
 &\leq \frac{1}{2\alpha_0} \|x_1 - x\|_\epsilon^2 + \sum_{t=1}^{T-1} \frac{\alpha_t}{2} \left\| \hat{v}_t^{-1/2} m_t \right\|_{\hat{v}_t^{1/2}}^2 \\
 &\quad + \frac{D_\infty^2}{2} \sum_{i=1}^d \left(\frac{\hat{v}_{T-1,i}^{1/2}}{\alpha_{T-1}} - \frac{\epsilon}{\alpha_0} \right) \\
 &= \frac{\epsilon^2}{2\alpha_0} \|x_1 - x\|^2 + \sum_{t=1}^{T-1} \frac{\alpha_t}{2} \left\| \hat{v}_t^{-1/2} m_t \right\|_{\hat{v}_t^{1/2}}^2 \\
 &\quad + \frac{D_\infty^2}{2\alpha_{T-1}} \sum_{i=1}^d \left(\hat{v}_{T-1,i}^{1/2} \right) - \frac{d\epsilon}{2\alpha_0} \\
 &\leq \frac{\epsilon^2}{2\alpha_0} \|x_1 - x\|^2 + \sum_{t=1}^{T-1} \frac{\alpha_t}{2} \left\| \hat{v}_t^{-1/2} m_t \right\|_{\hat{v}_t^{1/2}}^2 \\
 &\quad + \frac{D_\infty^2}{2\alpha_{T-1}} \sum_{i=1}^d \left(\hat{v}_{T-1,i}^{1/2} \right)
 \end{aligned}$$

where we have used $\hat{v}_0 = v_0 = \epsilon^2$ in the first term of the right hand side, so that $\|x\|_{\hat{v}_0^{1/2}}^2 = \epsilon^2 \|x\|_2^2 = \epsilon^2 \|x\|^2$. Finally, by noticing $\left\| \hat{v}_t^{-1/2} m_t \right\|_{\hat{v}_t^{1/2}}^2 = \|m_t\|_{\hat{v}_t^{-1/2}}^2$, we therefore have:

$$R_{1,t} \leq \frac{\epsilon^2}{2\alpha_0} \|x_1 - x\|^2 + \frac{D_\infty^2}{2\alpha_{T-1}} \sum_{i=1}^d \left(\hat{v}_{T-1,i}^{1/2} \right) + \frac{1}{2} \sum_{t=1}^{T-1} \alpha_t \|m_t\|_{\hat{v}_t^{-1/2}}^2 \quad (41)$$

B.2.2. BOUND OF $R_{2,t}$

$$R_{2,t} = - \sum_{t=1}^T \frac{1-\tau_t}{\tau_t} \langle m_{t-1}, x_t - x_{t-1} \rangle = \sum_{t=1}^T \frac{1-\tau_t}{\tau_t} \langle m_{t-1}, x_{t-1} - x_t \rangle = \sum_{t=1}^T \left\langle \frac{1-\tau_t}{\tau_t} m_{t-1}, x_{t-1} - x_t \right\rangle$$

with $\tilde{m}_{t-1} = \frac{1-\tau_t}{\tau_t} m_{t-1}$ and by using $m_0 = 0$, we have:

$$R_{2,t} = \sum_{t=1}^T \langle \tilde{m}_{t-1}, x_{t-1} - x_t \rangle = \sum_{t=2}^T \langle \tilde{m}_{t-1}, x_{t-1} - x_t \rangle = \sum_{t=1}^{T-1} \langle \tilde{m}_t, x_t - x_{t+1} \rangle$$

Then, by applying Holder's inequality, followed by the use of the projection operator where $x_t = \Pi_{\chi, \hat{v}_t^{1/2}}(x_t)$, since $x_t \in \chi$, we obtain:

$$R_{2,t} \leq \sum_{t=1}^{T-1} \|\tilde{m}_t\|_{\hat{v}_t^{-1/2}} \|x_t - x_{t+1}\|_{\hat{v}_t^{1/2}} = \sum_{t=1}^{T-1} \|\tilde{m}_t\|_{\hat{v}_t^{-1/2}} \left\| \Pi_{\chi, \hat{v}_t^{1/2}}(x_t) - \Pi_{\chi, \hat{v}_t^{1/2}}(x_t - \alpha_t \hat{v}_t^{-1/2} m_t) \right\|_{\hat{v}_t^{1/2}}$$

The non-expansive property of the operator then allows:

$$\begin{aligned}
 R_{2,t} &\leq \sum_{t=1}^{T-1} \|\tilde{m}_t\|_{\hat{v}_t^{-1/2}} \|x_t - x_{t+1}\|_{\hat{v}_t^{1/2}} \\
 &\leq \sum_{t=1}^{T-1} \|\tilde{m}_t\|_{\hat{v}_t^{-1/2}} \left\| x_t - (x_t - \alpha_t \hat{v}_t^{-1/2} m_t) \right\|_{\hat{v}_t^{1/2}} = \sum_{t=1}^{T-1} \|\tilde{m}_t\|_{\hat{v}_t^{-1/2}} \left\| \alpha_t \hat{v}_t^{-1/2} m_t \right\|_{\hat{v}_t^{1/2}} \\
 &= \sum_{t=1}^{T-1} \alpha_t \|\tilde{m}_t\|_{\hat{v}_t^{-1/2}} \|m_t\|_{\hat{v}_t^{-1/2}}
 \end{aligned}$$

Finally, using the upper bound in Eq. (28) and simplifying the d , we have:

$$R_{2,t} \leq \sum_{t=1}^{T-1} \alpha_t \frac{1 - \tau_t}{\tau_t} \|m_t\|_{\hat{v}_t^{-1/2}}^2 \leq \frac{\beta \tilde{\nu}_c + 4\epsilon^{-2} G_\infty^2}{\tilde{\nu}_c} \sum_{t=1}^{T-1} \alpha_t \|m_t\|_{\hat{v}_t^{-1/2}}^2 \quad (42)$$

B.2.3. BOUND OF $R_{3,t}$

$$\begin{aligned}
 R_{3,t} &= \sum_{t=1}^T \frac{1}{\tau_t} (\langle m_t, x_t - x \rangle - \langle m_{t-1}, x_{t-1} - x \rangle) = \sum_{t=1}^T A_t \\
 A_t &= \frac{1}{\tau_t} \langle m_t, x_t - x \rangle - \frac{1}{\tau_{t-1}} \langle m_{t-1}, x_{t-1} - x \rangle + \left(\frac{\tau_t - \tau_{t-1}}{\tau_t \tau_{t-1}} \right) \langle m_{t-1}, x_{t-1} - x \rangle \\
 &\leq \frac{1}{\tau_t} \langle m_t, x_t - x \rangle - \frac{1}{\tau_{t-1}} \langle m_{t-1}, x_{t-1} - x \rangle + \left(\frac{|\tau_t - \tau_{t-1}|}{\tau_t \tau_{t-1}} \right) \|m_{t-1}\|_1 \|x_{t-1} - x\|_\infty \\
 &\leq \frac{1}{\tau_t} \langle m_t, x_t - x \rangle - \frac{1}{\tau_{t-1}} \langle m_{t-1}, x_{t-1} - x \rangle + \left(\frac{|\tau_t - \tau_{t-1}|}{\tau_t \tau_{t-1}} \right) dD_\infty G_\infty \\
 &\leq \frac{1}{\tau_t} \langle m_t, x_t - x \rangle - \frac{1}{\tau_{t-1}} \langle m_{t-1}, x_{t-1} - x \rangle + \left((1 - \beta) - \frac{(1 - \beta)\tilde{\nu}_c}{\tilde{\nu}_c + 4\epsilon^{-2} G_\infty^2} \right) \left(\frac{\tilde{\nu}_c + 4\epsilon^{-2} G_\infty^2}{(1 - \beta)\tilde{\nu}_c} \right)^2 dD_\infty G_\infty
 \end{aligned}$$

Where we have made use of Holder's inequality (with $(p, q) = (1, \infty)$) and the bounds $\|m_{t-1}\|_1 \leq dG_\infty \|x_t - x\|_\infty \leq D_\infty$ in the third and fourth lines. The last line is obtained through the bounds of τ_t in Eq. (26) (with simplification of d). Finally, using the telescoping sum over the first two terms in A_t and with $m_0 = 0$, we arrive at the following relation:

$$R_{3,t} \leq \frac{1}{\tau_T} \langle m_T, x_T - x \rangle + \left(\frac{(1 - \beta)4\epsilon^{-2} G_\infty^2}{\tilde{\nu}_c + 4\epsilon^{-2} G_\infty^2} \right) \left(\frac{\tilde{\nu}_c + 4\epsilon^{-2} G_\infty^2}{(1 - \beta)\tilde{\nu}_c} \right)^2 dTD_\infty G_\infty \quad (43)$$

$$\begin{aligned}
 &\leq \frac{\tilde{\nu}_c + 4\epsilon^{-2} G_\infty^2}{(1 - \beta)\tilde{\nu}_c} |\langle m_T, x_T - x \rangle| + \left(\frac{(1 - \beta)4\epsilon^{-2} G_\infty^2}{\tilde{\nu}_c + 4\epsilon^{-2} G_\infty^2} \right) \left(\frac{\tilde{\nu}_c + 4\epsilon^{-2} G_\infty^2}{(1 - \beta)\tilde{\nu}_c} \right)^2 dTD_\infty G_\infty \\
 &\leq \left[\frac{\tilde{\nu}_c + 4\epsilon^{-2} G_\infty^2}{(1 - \beta)\tilde{\nu}_c} + \left(\frac{(1 - \beta)4\epsilon^{-2} G_\infty^2}{\tilde{\nu}_c + 4\epsilon^{-2} G_\infty^2} \right) \left(\frac{\tilde{\nu}_c + 4\epsilon^{-2} G_\infty^2}{(1 - \beta)\tilde{\nu}_c} \right)^2 T \right] dD_\infty G_\infty \quad (44)
 \end{aligned}$$

B.2.4. BOUND OF $\sum_{t=1}^{T-1} \alpha_t \|m_t\|_{\hat{v}_t^{-1/2}}^2$

With

$$m_t = (1 - \tau_t)m_{t-1} + \tau_t g_t = \sum_{k=1}^t \tau_k g_k \prod_{j=1}^{t-k} (1 - \tau_{t-j+1})$$

we have:

$$\begin{aligned}
 \sum_{t=1}^{T-1} \alpha_t \|m_t\|_{\hat{v}_t^{-1/2}}^2 &= \sum_{t=1}^{T-1} \alpha_t \left\| \hat{v}_t^{-1/4} m_t \right\|_2^2 = \sum_{t=1}^{T-2} \alpha_t \left\| \hat{v}_t^{-1/4} m_t \right\|_2^2 + \alpha_{T-1} \left\| \hat{v}_{T-1}^{-1/4} m_{T-1} \right\|_2^2 \\
 &\leq \sum_{t=1}^{T-2} \alpha_t \left\| \hat{v}_t^{-1/4} m_t \right\|_2^2 + \frac{\alpha_{T-1}}{\epsilon} \|m_{T-1}\|^2 \\
 &= \sum_{t=1}^{T-2} \alpha_t \left\| \hat{v}_t^{-1/4} m_t \right\|_2^2 + \frac{\alpha}{\epsilon \sqrt{T-1}} \sum_{i=1}^d \left(\sum_{t=1}^{T-1} \tau_t g_{t,i} \prod_{j=1}^{T-1-t} (1 - \tau_{T-j}) \right)^2 \\
 &\leq \sum_{t=1}^{T-2} \alpha_t \left\| \hat{v}_t^{-1/4} m_t \right\|_2^2 + \frac{\alpha}{\epsilon \sqrt{T-1}} \sum_{i=1}^d \left(\sum_{t=1}^{T-1} \tau_t |g_{t,i}| \prod_{j=1}^{T-1-t} (1 - \tau_{T-j}) \right)^2
 \end{aligned}$$

Since $\tau_t \leq (1 - \beta)$ and $(1 - \tau_t) \leq B = \frac{\beta \bar{\nu}_c + 4\epsilon^{-2} G_\infty^2}{\bar{\nu}_c + 4\epsilon^{-2} G_\infty^2}$, we can write:

$$\begin{aligned}
 \sum_{t=1}^{T-1} \alpha_t \|m_t\|_{\hat{v}_t^{-1/2}}^2 &\leq \sum_{t=1}^{T-2} \alpha_t \left\| \hat{v}_t^{-1/4} m_t \right\|_2^2 + \frac{\alpha(1 - \beta)^2}{\epsilon \sqrt{T-1}} \sum_{i=1}^d \left(\sum_{t=1}^{T-1} |g_{t,i}| \prod_{j=1}^{T-1-t} B \right)^2 \\
 &= \sum_{t=1}^{T-2} \alpha_t \left\| \hat{v}_t^{-1/4} m_t \right\|_2^2 + \frac{\alpha(1 - \beta)^2}{\epsilon \sqrt{T-1}} \sum_{i=1}^d \left(\sum_{t=1}^{T-1} |g_{t,i}| B^{T-1-t} \right)^2 \\
 &\leq \sum_{t=1}^{T-2} \alpha_t \left\| \hat{v}_t^{-1/4} m_t \right\|_2^2 + \frac{\alpha(1 - \beta)^2}{\epsilon \sqrt{T-1}} \sum_{i=1}^d \left(\sum_{t=1}^{T-1} B^{T-1-t} \right) \left(\sum_{t=1}^{T-1} B^{T-1-t} g_{t,i}^2 \right)
 \end{aligned}$$

where we have used Cauchy-Schwartz's inequality $\langle u, v \rangle^2 \leq \|u\|^2 \|v\|^2$ with $u_t = \sqrt{B^{T-1-t}}$ and $v_t = \sqrt{B^{T-1-t}} |g_{t,i}|$.

We therefore have:

$$\begin{aligned}
 & \sum_{t=1}^{T-1} \alpha_t \|m_t\|_{\hat{v}_t}^2 \\
 & \leq \sum_{t=1}^{T-2} \alpha_t \left\| \hat{v}_t^{-1/4} m_t \right\|^2 + \frac{\alpha(1-\beta)^2}{\epsilon \sqrt{T-1}} \sum_{i=1}^d \frac{(1-B^{T-1})}{(1-B)} \sum_{t=1}^{T-1} B^{T-1-t} g_{t,i}^2 \\
 & \leq \sum_{t=1}^{T-2} \alpha_t \left\| \hat{v}_t^{-1/4} m_t \right\|^2 + \frac{\alpha(1-\beta)^2}{\epsilon(1-B)} \sum_{i=1}^d \sum_{t=1}^{T-1} B^{T-1-t} g_{t,i}^2 \frac{1}{\sqrt{T-1}} \\
 & \leq \sum_{t=1}^{T-1} \frac{\alpha(1-\beta)^2}{\epsilon(1-B)} \sum_{i=1}^d \sum_{j=1}^t B^{t-j} g_{j,i}^2 \frac{1}{\sqrt{t}} = \frac{\alpha(1-\beta)^2}{\epsilon(1-B)} \sum_{t=1}^{T-1} \sum_{i=1}^d \sum_{j=1}^t B^{t-j} g_{j,i}^2 \frac{1}{\sqrt{t}} \\
 & = \frac{\alpha(1-\beta)^2}{\epsilon(1-B)} \sum_{i=1}^d \sum_{t=1}^{T-1} g_{t,i}^2 \sum_{j=t}^{T-1} B^{j-t} \frac{1}{\sqrt{j}} \\
 & \leq \frac{\alpha(1-\beta)^2}{\epsilon(1-B)} \sum_{i=1}^d \sum_{t=1}^{T-1} g_{t,i}^2 \sum_{j=t}^{T-1} B^{j-t} \frac{1}{\sqrt{t}} \\
 & = \frac{\alpha(1-\beta)^2}{\epsilon(1-B)} \sum_{i=1}^d \sum_{t=1}^{T-1} \frac{g_{t,i}^2}{\sqrt{t}} \sum_{j=t}^{T-1} B^{j-t} = \frac{\alpha(1-\beta)^2}{\epsilon(1-B)} \sum_{i=1}^d \sum_{t=1}^{T-1} \frac{g_{t,i}^2}{\sqrt{t}} \left(\frac{1-B^{T-t}}{1-B} \right) \\
 & \leq \frac{\alpha(1-\beta)^2}{\epsilon(1-B)^2} \sum_{i=1}^d \sum_{t=1}^{T-1} \frac{g_{t,i}^2}{\sqrt{t}} \quad (\text{Since } (1-B^{T-t}) < 1)
 \end{aligned}$$

Finally, using Cauchy-Schwartz's inequality (without the squares) once more with $u_t = g_{t,i}^2$ and $v_t = \frac{1}{\sqrt{t}}$, and with

$\sum_{t=1}^{T-1} \frac{1}{t} \leq 1 + \log(T-1)$, we get:

$$\sum_{t=1}^{T-1} \alpha_t \|m_t\|_{\hat{v}_t}^2 \leq \frac{\alpha(1-\beta)^2}{\epsilon(1-B)^2} \sum_{i=1}^d \|g_{1:T-1,i}^2\|_2 \sqrt{\sum_{t=1}^{T-1} \frac{1}{t}} \leq \frac{\alpha(1-\beta)^2}{\epsilon(1-B)^2} \sum_{i=1}^d \|g_{1:T-1,i}^2\|_2 \sqrt{1 + \log(T-1)}$$

By using the fact that

$$1 - B = \frac{(1-\beta)\tilde{\nu}_c}{\tilde{\nu}_c + 4\epsilon^{-2}G_\infty^2} \Leftrightarrow \frac{1}{(1-B)^2} = \left(\frac{\tilde{\nu}_c + 4\epsilon^{-2}G_\infty^2}{(1-\beta)\tilde{\nu}_c} \right)^2 \quad (45)$$

we obtain the final bound:

$$\sum_{t=1}^{T-1} \alpha_t \|m_t\|_{\hat{v}_t}^2 \leq \frac{\alpha \sqrt{1 + \log(T-1)}}{\epsilon} \left(\frac{\tilde{\nu}_c + 4\epsilon^{-2}G_\infty^2}{\tilde{\nu}_c} \right)^2 \sum_{i=1}^d \|g_{1:T-1,i}^2\|_2 \quad (46)$$

B.2.5. BOUND OF THE REGRET

$$\begin{aligned}
 \sum_{t=1}^T \langle g_t, x_t - x \rangle &= R_{1,t} + R_{2,t} + R_{3,t} \\
 R_{1,t} &= \sum_{t=1}^T \langle m_{t-1}, x_{t-1} - x \rangle \\
 &\leq \frac{\epsilon^2}{2\alpha_0} \|x_1 - x\|^2 + \frac{D_\infty^2}{2\alpha_{T-1}} \sum_{i=1}^d \left(\hat{v}_{T-1,i}^{1/2} \right) + \frac{1}{2} \sum_{t=1}^{T-1} \alpha_t \|m_t\|_{\hat{v}_t^{-1/2}}^2 \\
 &\leq \frac{\epsilon^2}{2\alpha_0} \|x_1 - x\|^2 + \frac{D_\infty^2}{2\alpha_{T-1}} \sum_{i=1}^d \left(\hat{v}_{T-1,i}^{1/2} \right) \\
 &\quad + \frac{1}{2} \frac{\alpha \sqrt{1 + \log(T-1)}}{\epsilon} \left(\frac{\tilde{\nu}_c + 4\epsilon^{-2} G_\infty^2}{\tilde{\nu}_c} \right)^2 \sum_{i=1}^d \|g_{1:T-1,i}^2\|_2 \\
 R_{2,t} &= - \sum_{t=1}^T \frac{1 - \tau_t}{\tau_t} \langle m_{t-1}, x_t - x_{t-1} \rangle \\
 &\leq \frac{\beta \tilde{\nu}_c + 4\epsilon^{-2} G_\infty^2}{\tilde{\nu}_c} \sum_{t=1}^{T-1} \alpha_t \|m_t\|_{\hat{v}_t^{-1/2}}^2 \\
 &\leq \frac{\alpha \sqrt{1 + \log(T-1)}}{\epsilon} \left(\frac{\beta \tilde{\nu}_c + 4\epsilon^{-2} G_\infty^2}{\tilde{\nu}_c} \right) \left(\frac{\tilde{\nu}_c + 4\epsilon^{-2} G_\infty^2}{\tilde{\nu}_c} \right)^2 \sum_{i=1}^d \|g_{1:T-1,i}^2\|_2 \\
 R_{3,t} &= \sum_{t=1}^T \frac{1}{\tau_t} (\langle m_t, x_t - x \rangle - \langle m_{t-1}, x_{t-1} - x \rangle) \\
 &\leq \left[\frac{\tilde{\nu}_c + 4\epsilon^{-2} G_\infty^2}{(1 - \beta) \tilde{\nu}_c} + \left(\frac{(1 - \beta) 4\epsilon^{-2} G_\infty^2}{\tilde{\nu}_c + 4\epsilon^{-2} G_\infty^2} \right) \left(\frac{\tilde{\nu}_c + 4\epsilon^{-2} G_\infty^2}{(1 - \beta) \tilde{\nu}_c} \right)^2 T \right] d D_\infty G_\infty
 \end{aligned}$$

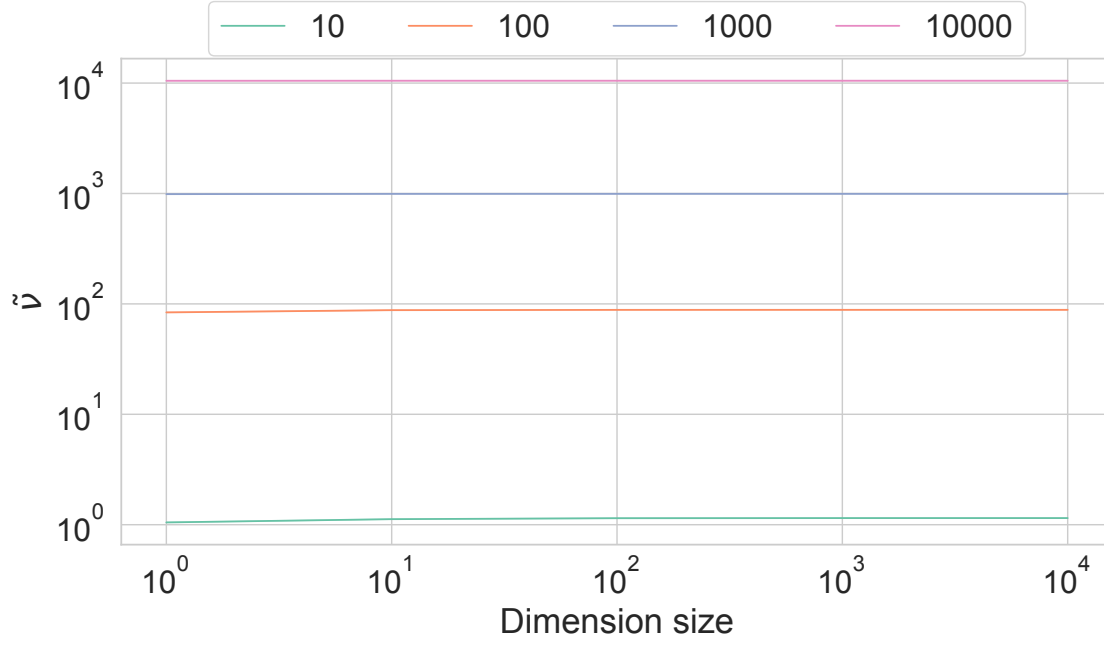
We therefore have:

$$\begin{aligned}
 \sum_{t=1}^T f_t(x_t) - f_t(x^*) &\leq \frac{\epsilon^2}{2\alpha_0} \|x_1 - x^*\|^2 + \frac{D_\infty^2}{2\alpha_{T-1}} \sum_{i=1}^d \left(\hat{v}_{T-1,i}^{1/2} \right) \\
 &\quad + \left(\frac{1}{2} + \frac{\beta \tilde{\nu}_c + 4\epsilon^{-2} G_\infty^2}{\tilde{\nu}_c} \right) \frac{\alpha \sqrt{1 + \log(T-1)}}{\epsilon} \left(\frac{\tilde{\nu}_c + 4\epsilon^{-2} G_\infty^2}{\tilde{\nu}_c} \right)^2 \sum_{i=1}^d \|g_{1:T-1,i}^2\|_2 \quad (47) \\
 &\quad + \left[\frac{\tilde{\nu}_c + 4\epsilon^{-2} G_\infty^2}{(1 - \beta) \tilde{\nu}_c} + \left(\frac{(1 - \beta) 4\epsilon^{-2} G_\infty^2}{\tilde{\nu}_c + 4\epsilon^{-2} G_\infty^2} \right) \left(\frac{\tilde{\nu}_c + 4\epsilon^{-2} G_\infty^2}{(1 - \beta) \tilde{\nu}_c} \right)^2 T \right] d D_\infty G_\infty
 \end{aligned}$$

 B.3. Expected $\tilde{\nu}_c$

As mentioned before, in the non-convergent period ($1 \leq t \leq \hat{T} \leq T$), $\tilde{\nu}_c$ is given as $\tilde{\nu}$. We consider $\tilde{\nu}_c$ in the convergent period, especially when \mathcal{D} contains almost no noise and outliers.

With respect to the central limit theorem, we can assume that the gradients g_t are ultimately generated from asymptotic normal distribution as $t \rightarrow \infty$. In that case, $dD = \{(g_t - m_{t-1})^2\}^\top v_{t-1}^{-1}$ is expected to follow the chi-squared distribution with d the degrees of freedom. We then obtain the convergence point of $\tilde{\nu}$ ($= \tilde{\nu}_c$) from the numerical solution, as shown in Fig. 4. From this result, if \mathcal{D} contains almost no noise, $\tilde{\nu}_c \rightarrow \infty$ is expected. Hence, the regret bound of AdaTerm can be


 Figure 4. Convergence behavior of $\tilde{\nu}$ (legends denote the number of updates)

divided as follows:

$$\begin{aligned}
 \sum_{t=1}^T f_t(x_t) - f_t(x^*) &= \sum_{t=1}^{\hat{T}} f_t(x_t) - f_t(x^*) + \sum_{t=\hat{T}+1}^T f_t(x_t) - f_t(x^*) \\
 &\leq \frac{\epsilon^2}{2\alpha_0} \|x_1 - x^*\|^2 + \frac{D_\infty^2}{2\alpha_{\hat{T}-1}} \sum_{i=1}^d \left(\hat{v}_{\hat{T}-1,i}^{1/2} \right) \\
 &\quad + \left(\frac{1}{2} + \frac{\beta \tilde{\nu} + 4\epsilon^{-2}G_\infty^2}{\tilde{\nu}} \right) \frac{\alpha \sqrt{1 + \log(\hat{T} - 1)}}{\epsilon} \left(\frac{\tilde{\nu} + 4\epsilon^{-2}G_\infty^2}{\tilde{\nu}} \right)^2 \sum_{i=1}^d \|g_{1:\hat{T}-1,i}^2\|_2 \\
 &\quad + \frac{1}{\tau_{\hat{T}}} \langle m_{\hat{T}}, x_{\hat{T}} - x^* \rangle + \left(\frac{(1-\beta)4\epsilon^{-2}G_\infty^2}{\tilde{\nu} + 4\epsilon^{-2}G_\infty^2} \right) \left(\frac{\tilde{\nu} + 4\epsilon^{-2}G_\infty^2}{(1-\beta)\tilde{\nu}} \right)^2 d\hat{T}D_\infty G_\infty \\
 &\quad + \frac{\epsilon^2}{2\alpha_{\hat{T}}} \|x_{\hat{T}+1} - x^*\|^2 + \frac{D_\infty^2}{2\alpha_{T-1}} \sum_{i=1}^d \left(\hat{v}_{T-1,i}^{1/2} \right) + \frac{1}{1-\beta} (\langle m_T, x_T - x^* \rangle - \langle m_{\hat{T}}, x_{\hat{T}} - x^* \rangle) \\
 &\quad + \left(\frac{1}{2} + \beta \right) \frac{\alpha \sqrt{1 + \log(T - \hat{T} - 1)}}{\epsilon} \sum_{i=1}^d \|g_{\hat{T}+1:T-1,i}^2\|_2
 \end{aligned} \tag{48}$$

Where we used the upper bound of $R_{3,t}$ from Eq. (43) instead of the one in Eq. (44). If we can minimize $\hat{T} \rightarrow 0$, i.e. the initial value of $\tilde{\nu}$ is set to be almost ∞ and it is the near-optimal convergent value, we can get the regret bound only with the last two lines remaining, which is similar to the bound of other optimizers.

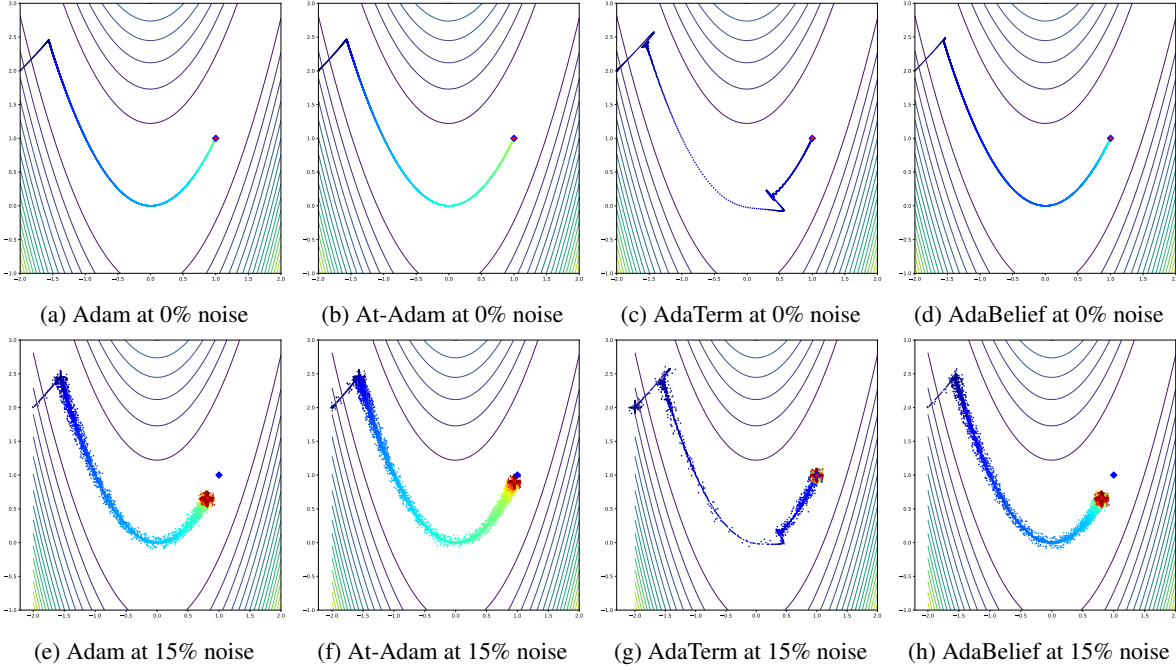


Figure 5. Trajectories on Rosenbrock function

C. Details of test functions

The test functions tested $f(x, y)$ were Rosenbrock with a valley, McCormick with a plate, and Michalewicz with steep drops, as defined below.

$$f(x, y) = \begin{cases} 100(y - x^2)^2 + (x - 1)^2 & \text{Rosenbrock} \\ \sin(x + y) + (x - y)^2 - 1.5x + 2.5y + 1 & \text{McCormick} \\ -\sin(x) \sin^{20}(x^2/\pi) - \sin(y) \sin^{20}(2y^2/\pi) & \text{Michalewicz} \end{cases} \quad (49)$$

Using the gradients of $f(x, y)$, (x, y) can be optimized to minimize $f(x, y)$. The initial values of (x, y) were fixed to $(-2, 2)$, $(4, -3)$, and $(1, 1)$, respectively. The noise added to (x, y) for computing the gradients was sampled from the uniform distribution with range $(-0.1, 0.1)$. The probability of noise was set to six conditions: $\{0, 1, 2.5, 5, 10, 15\}\%$.

The optimizers tested were Adam, At-Adam with adaptive ν , and the proposed AdaTerm. AdaBelief (Zhuang et al., 2020), which is similar to AdaTerm with $\nu \rightarrow \infty$, was also tested, but was excluded from Figs. 2 and 3 due to its similarity to Adam. The learning rate was set to $\alpha = 0.01$, which is higher than that for typical network updates, but other hyper-parameters were left at their default settings. The update was performed 15000 times and the error norm between the final (x, y) and the analytically-optimal point was computed. To evaluate the statistics, 100 trials were run with different random seeds.

Trajectories of the convergence process are illustrated in Figs. 5–7. Note that the color of each point indicates the elapsed time, changing from blue to red. AdaTerm was less likely to update in the wrong direction caused by noise than the others, indicating stable updating as well as the cases with almost no noise. In addition, we found the faster update speed of AdaTerm than others. This is probably because $\beta < \beta_2$ could quickly adapt to small gradients in the saddle area, although this caused the overshoot around the optimal point in Fig. 6c, resulting in the larger error norm than the others in Fig. 2.

A remarkable result was obtained for Michalewicz function (see Fig. 7c). Specifically, AdaTerm initially moved only in the y -direction, as in AdaBelief, and then paused at steep gradients in the x -direction. This is because the steep gradients toward the optimum were considered as noise for a while. In fact, as time passed, AdaTerm judged that the steep gradients are not noise. Then, as $\tilde{\nu}$ became larger, the update was resumed, finally reaching the optimal point. On the other hand, At-Adam was unable to adapt ν to the steep gradients, and the point moved to avoid the optimal point (see Fig. 7b). When noise was added, however, the steep gradients started to be utilized with the help of noise, and the optimal point was finally reached.

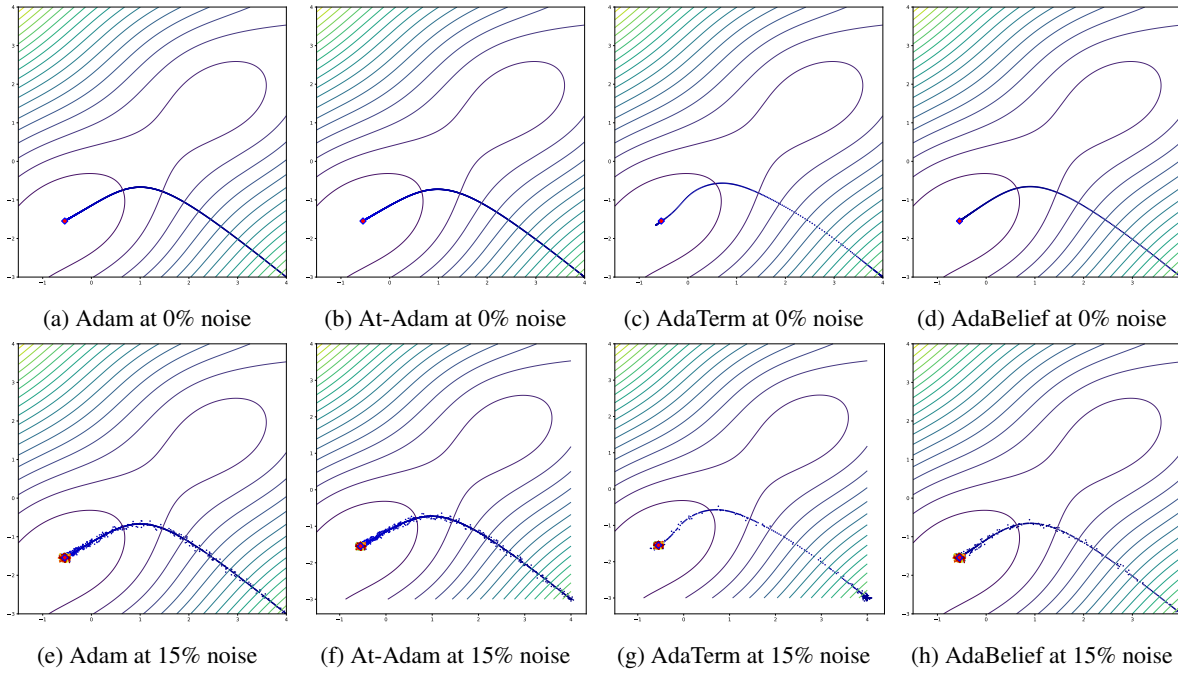


Figure 6. Trajectories on McCormick function

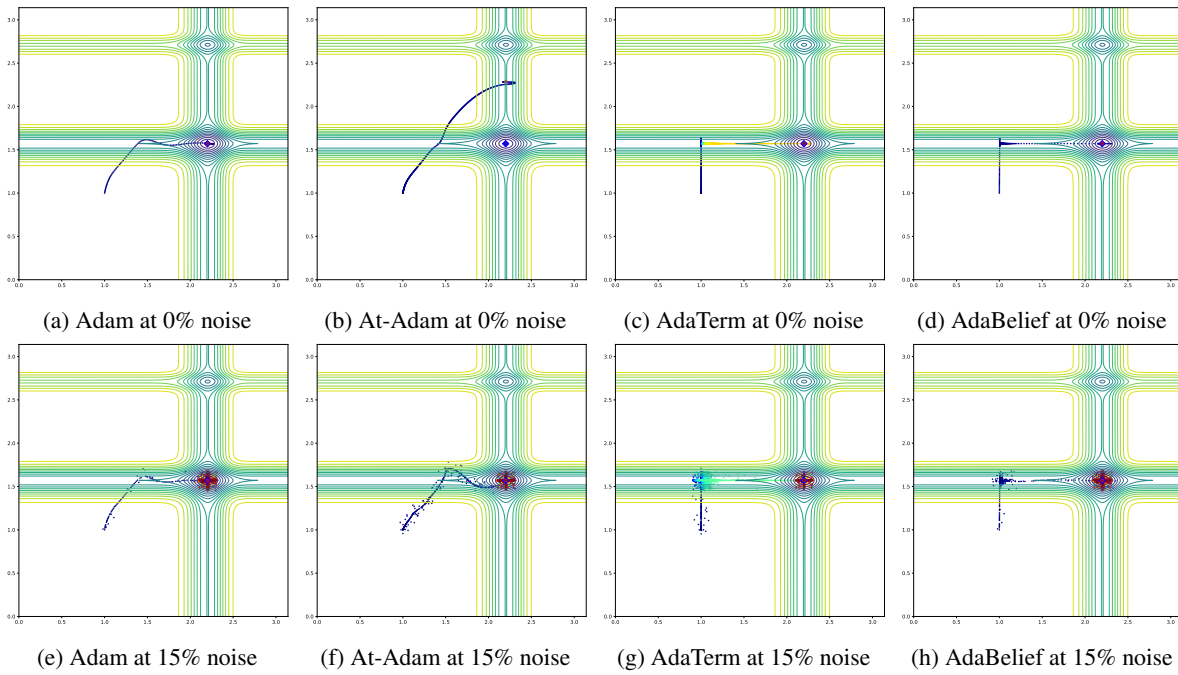


Figure 7. Trajectories on Michalewicz function

Table 2. Learning setups

Parameter	Classification	Prediction	RL	Distillation
Learning rate	1e-3	1e-3	1e-4	1e-3
Batch size	256	32	32	32
#Epoch	100	100/300	2000	200
Label smoothing	0.2	-	-	-
Truncation	-	30	-	-
#Batch/#Replay buffer	-	-	128/1e+4	-
Weight decay	-	-	-	1e-4

D. Learning setups

The models for learning the four benchmark problems are implemented using PyTorch (Paszke et al., 2017) with the respective setups, as summarized in Table 2. The parameters that are not listed in the table are basically set to be the recommended default values. Note that the learning rate for RL was smaller than ones for the other problems to avoid getting stuck in one of the local solutions before good samples are collected. In addition, the batch size was basically kept 32 to make the noise more likely to affect the gradients, but for the classification problem only, the batch size was increased to 256, which is within the general range, due to the too increased learning cost.

For the classification problem, ResNet18 (He et al., 2016) was employed as the network model. The official PyTorch implementation was basically employed, but to take the size difference of the input image into account, the first layer of convolution was changed to one with kernel size of 3 and stride of 1 and the subsequent MaxPool layer was excluded.

For the prediction problem, a gated recurrent unit (GRU) (Chung et al., 2014) was employed for constructing the network model, which consists of two serial hidden layers with each holding 128 GRU units. In the output layer, the state-dimensional means and standard deviations, which are parameters of the multivariate diagonal Gaussian distribution, are outputted. Note that, since extending the number of prediction steps delays the learning process, we set the epoch to 100 for 1-step prediction and 300 for 30-step prediction.

For the RL problem, five fully-connected layers with 100 neurons for each were implemented as the hidden layers. Each activation function was an unlearned LayerNorm (Ba et al., 2016; Xu et al., 2019) and Swish function (Elfwing et al., 2018). The output is a multivariate diagonal student’s t-distribution to improve the efficiency of the exploration (Kobayashi, 2019).

For the policy distillation problem, two fully-connected layers with only 32 neurons for each were implemented as the hidden layers. This structure is clearly smaller than that for the RL problem described above. Each activation function was only Tanh function, with reference to the fact that this design has been reported to have sufficient expressive capability (De Ryck et al., 2021). In the output layer, the state-dimensional means and standard deviations, which are parameters of the multivariate diagonal Gaussian distribution, are outputted.

Table 3. Ablation results

Method	Classification		Prediction		RL		Distillation	
	Accuracy		MSE at final prediction		The sum of rewards		The sum of rewards	
	0 %	10 %	1 step	30 steps	Hopper	Ant	w/o amateur	w/ amateur
AdaTerm	0.731 (3.7e-3)	0.682 (4.5e-3)	0.034 (5.6e-4)	0.907 (1.4e-1)	1705 (6.3e+2)	1986 (3.8e+2)	1737 (2.0e+2)	1528 (1.6e+2)
No adaptiveness	0.733 (3.2e-3)	0.684 (4.2e-3)	0.037 (5.3e-4)	0.937 (2.1e-1)	325 (3.6e+2)	2220 (3.0e+2)	1714 (1.8e+2)	1319 (3.0e+2)
No robustness	0.733 (3.2e-3)	0.681 (3.8e-3)	0.033 (4.0e-4)	1.216 (1.3e-1)	1634 (5.4e+2)	1229 (6.6e+2)	1678 (2.3e+2)	1485 (2.4e+2)
Large init	0.735 (3.5e-3)	0.683 (3.9e-3)	0.033 (4.9e-4)	1.203 (1.2e-1)	1527 (6.6e+2)	1845 (2.9e+2)	1645 (2.7e+2)	1435 (2.4e+2)

E. Ablation study

For the ablation test of AdaTerm, we test the following three conditions: $\Delta\tilde{\nu} = 0$, called no adaptiveness; $\tilde{\nu} = \infty$, called no robustness; and $\tilde{\nu}_0 = 100$, called large init. All other conditions are the same as the experiments in the main text.

The test results are summarized in Table 3. As expected mostly, the no adaptiveness outperformed the no robustness for the problems with high noise effects; and vice versa. From the results of such as the 30-step prediction and the policy distillation, we can say that the optimal solution may lie somewhere in the middle, rather than at the two extremes, and the normal AdaTerm found them. On the other hand, in the case where $\tilde{\nu}_0$ is increased and the noise robustness is poor at the beginning of training, the performance was worse than the normal case where $\tilde{\nu}_0 = \tilde{\nu} + \epsilon$ and the noise robustness is maximized at the beginning, except for the classification problem. This tendency suggests that even if $\tilde{\nu}$ is adjusted to gain the appropriate noise robustness after optimization without considering the effects of noise, the performance would be prone to get stuck in one of the local solutions. For the classification problem only, the size of the network architecture was larger than ones for the other problems, and its redundancy allowed the classifier to escape from the local solutions. In such a case, the more gradients utilized from the beginning resulted in the performance improvement.